Alice Fernandes Coutinho
BEng. in Chemical and Biochemical Engineering

Membrane Screening for Peptide Fragment Condensation

Dissertation to obtain the Master Degree in Chemical and Biochemical Engineering

Supervisor: Andrew Livingston, Professor of Chemical Engineering, Imperial College London

Co-Supervisor: João Paulo Crespo, Professor Catedrático, Universidade Nova de Lisboa

Júri:

Presidente: Prof. Doutor Mário Fernando José Eusébio
Arguente(s): Doutora Carla Alexandra Moreira Portugal
Vogal(ais): Prof. Doutor João Paulo Serejo Goulão Crespo

FACULDADE DE CIÊNCIAS E TECNOLOGIA
UNIVERSIDADE NOVA DE LISBOA

September 2019

Alice Fernandes Coutinho
BEng. in Chemical and Biochemical Engineering

Membrane Screening for Peptide Fragment Condensation

Dissertation to obtain the Master Degree in Chemical and Biochemical Engineering

Supervisor: Andrew Livingston, Prof. Dr., Imperial College London

Co-Supervisor: João Paulo Crespo, Prof. Dr., UNL

Degree in Association with

IMPERIAL COLLEGE LONDON
Faculty of Engineering
Department of Chemical Engineering and Chemical Technology

UNIVERSIDADE NOVA DE LISBOA
Faculdade de Ciências e Tecnologia
Departamento de Química

September 2019

Membrane Screening for Peptide Fragment Condensation

Acknowledgements

I would like to express my gratitude to the Imperial College of London and Professor Andrew Livingston for the opportunity to participate in the UROP programme.

I am deeply grateful to all the colleagues of Professor Livingston's group, as well as, Dr Ludmila Peeva and PhD student Jet Yeo that worked with me daily during the master research and dissertation writing.

I would also like to thanks to Professor José Paulo Mota for introducing me to Professor Andrew Livingston and Professor João Crespo my Portuguese co-supervisor

.

Resumo

Nesta tese apresenta-se uma prova de conceito de um processo de diafiltração para a purificação de ingredientes farmacêuticos ativos (APIs) integrando duas membranas de Nanofiltração por Solvente Orgânico (OSN). As soluções testadas incluíram PEG400, PEG1000, PEG2000, PEG8000 e PEG20000 em THF, pois os APIs têm um peso molecular (MW) de 8000Da e 20kDa, enquanto as impurezas e subprodutos variam até 2000Da.

Numa fase inicial, PBIj1000, PBIm5j2005, PEEK50, PEEK80 e membranas de polietileno (PE) modificadas com 2g/L ou 4g/L de polidopamina por 18h, 30h e 48h foram testadas em *single stage* a diferentes pressões. Os resultados mostram que o PE revestido com 2g/L de polidopamina apresenta rejeições abaixo de 50% para PEG2000 e acima de 85% para PEGs maiores, enquanto o PBIj1000 tem cerca de 78% de rejeição para PEG2000 e cerca de 98% para PEG8000 e PEG20000.

Os processos de cascata e diafiltração foram simulados no MATLAB para entender as condições de pressão de cada estágio. A partir dos resultados em cascata, o mais adequado para realizar a diafiltração foi PDA2g/L_30h a 20bar no primeiro estágio e PBIj1000 a 10bar no segundo estágio. A rejeição no segundo estágio foi 95% para PEG8000 e PEG20000 e 68% para PEG2000. Na primeira configuração para diafiltração, embora a curva de pureza experimental se ajuste ao modelo, o rendimento experimental para PEG8000 e PEG20k caiu para 10% após 6 vols, enquanto as previsões apontaram para 90%. No entanto, depois da alteração da configuração da diafiltração, substituindo o agitador magnético por agitação por bombas, o rendimento do produto experimental aumentou de 10% para 30%, como consequência do aumento dos efeitos da transferência de massa. A pureza experimental do produto foi menor que anteriormente e 10% inferior aos valores previstos pela simulação, atingindo 50% e 60% para PEG8000 e PEG20k, respectivamente.

Palavras-Chave: Membranas poliméricas, Purificação de APIs, Cascatas de Membranas, Diafiltração, Simulações em MATLAB

Abstract

This thesis is a proof of concept of a diafiltration process for the purification of active pharmaceutical ingredients (APIs) integrating two Organic Solvent Nanofiltration (OSN) membranes for a more efficient separation. The solutions tested included PEG400, PEG1000, PEG2000, PEG8000 and PEG20000 in THF due to the fact that the target APIs products have a molecular weight (MW) of 8000Da and 20kDa while the impurities and by-products range 2000Da.

In an initial phase PBIj1000, PBIm5j2005, PEEK50, PEEK80 and membranes based on polyethylene (PE) coating with 2g/L or 4g/L of polydopamine for 18h, 30, and 48h different were tested in a single stage mode at different pressures. The results show that PE coated with 2g/L of polydopamine presents rejections below 50% for PEG2000 and above 85% for larger PEGs, while PBIj1000 has about 78% rejection for PEG2000 and about 98% for PEG8000 and PEG20000.

It was necessary to simulate the cascade and diafiltration process in MATLAB in order to understand the pressure conditions for each stage. From the cascade results, the most suitable to perform diafiltration was PDA2g/L_30h at 20 bar in the first stage and PBIj1000 at 10 bar for the second stage, with the second stage rejecting about 95% PEG8000 and PEG20000, and 68% PEG2000. The first configuration for diafiltration, although the experimental purity curve fits the model prediction, the experimental yield for PEG8000 and PEG20k dropped to 10% after 6 vols while the predictions pointed to 90%. Nevertheless, once the diafiltration configuration was changed, by replacing the magnetic stirrer for agitation by pumps, the experimental product yield increased from 10% to 30%, as a consequence of an increase in mass transference effects. The experimental purity of the product was lower than previously and usually 10% lower than the simulation predictions reaching 50% and 60% for PEG8000 and PEG20k, respectively.

Keywords: Polymeric membranes, APIs purification, Membrane Cascades, Diafiltration, MATLAB Simulations

Contents Index

Illustration Index

Table Index

Equation Index

SPPS- Solid-phase peptide synthesis

OSN- Organic solvent nanofiltration

NF- Nanofiltration

PBI- Polybenzimidazole

THF- Tetrahydrofuran

DIC- N,N′-Diisopropylcarbodiimide

HOBt- Hydroxybenzotriazole

R- Retentate

P1- Permeate of the inlet side

P2- Permeate of the outlet side

PI- Phosphatidylinositol

HPLC- High Performance Liquid Chromatography

MeCN- Acetronitrile

FDA- Food and Drug Administration

PE- Polyethylene

PEEK- Poly(ether-ether-ketone)

SEM- Scanning Electron Microscope

RT- Retention Time

PBI- Polybenzimidazole

MW- Molecular Weight

API- Active Pharmaceutical Ingredient

Fmoc - 9-fluorenylmethoxycarbonyl

Boc- Tert-butoxycarbonyl

TBA- Trifluoracetic Acid

MSA- methanesulfonic acid

SA- sulphuric acid

DBX- dibromoxylene

ISA- Integrally Skinned Asymmetric (if not otherwise stated).

1 . Introduction and Scope of Thesis

In the pharmaceutical industry, the separation and purification of active pharmaceutical ingredients (APIs) account for about 40-70% of the total capital cost of the process (Spear, 2006). Therefore improving the efficiency of the process is crucial to minimize the production costs without compromising the quality of the product and the regulations that have to be obeyed in order to be commercialized. In a synthesis, intermediate products and the APIs have to be separated from the by-products and unreacted reagents. Usually, this by-products and unreacted reagents have a smaller molecular weight (MW) but they can also have higher MW. Technologies such as crystallization and column chromatography are usually used in purification, but these are expensive and difficult to control (Silva, 2012).

Organic Solvent Nanofiltration (OSN) is an emerging technology with the potential to separate different solutes based on their size and charge. This separation is achieved by the pressure difference across the membrane that retains the solute with higher MW and permeates the solute with smaller MW than the membrane pores. The advantage of this process compared with crystallization and column chromatography is that the energy consumption is lower and due to the fact that works at room temperature, thermal degradation and side reactions are avoided (Vandezande, 2008).

A typical example of API synthesis is a fragment condensation process of peptides as performed in the solution phase. A new concept for this process is based on assembling fragments of amino acids to a soluble polymer. In every step of the synthesis, it is necessary to purify the growing peptide from excess fragments and reagents by diafiltration processes. For the purification process, it is essential that membranes with appropriate separation properties are utilised in order to maximize peptide yield and purity.

Therefore, this thesis focuses on the selection of OSN membranes appropriate for the purification of peptide via fragment condensation. As a case study, it is selected synthesis of Glucagon via condensation of 4 fragments with MW of about 2000Da.

2 . Background and Literature Review

In this chapter, it will be presented the state of art of the membrane technology relevant to understanding the research and data that were collected and analysed.

2.1. Introduction to Membrane Technology

A membrane is a physical barrier between two distinct solutions, which allow selectively that some components pass through it. There are different separation mechanism based on different physical principles.

2.1.1 Nanofiltration and Organic Solvent Nanofiltration

Membranes are selective semi-permeable barriers and in recent years have been studied and used in separation and purification processes. These barriers separate the solutes in permeate and retentate according to their molecular weight, Figure 1. There is no rule concerning the retentate being or not being the desired product, due to the fact that the desired product can be the one with higher MW and be in the retentate or the one with smaller MW and be the permeate. Depending on the range of MW they can separate, membranes can be classified as reverse osmosis, nanofiltration, ultrafiltration and microfiltration. In this work, the OSN requires a nanofiltration membrane. (Mulder, Ch I Introduction, 1996) (R.W., 2004) One of the most important parameters that characterize the operating conditions of a membrane is the molecular weight cut-off (MWCO). The MWCO is a parameter that describes the operating range of the membrane and it's defined as the MW for which 90% of the solute is rejected by the membrane (See-Toh., 2008)

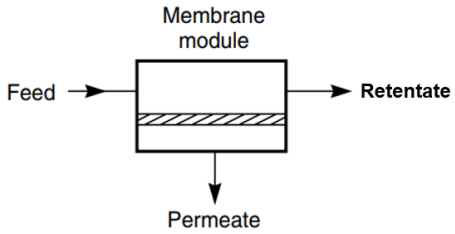

Figure 1. Schematic diagram of the basic membrane gas separation process (adapted from (R.W., 2004)

Nanofiltration (NF) was initially developed for water softening. Nowadays it's a separation method based on the size and molecular weight (MW) for molecules ranging from 100-2000 Da. The solute with smaller MW will be rejected by the membrane and will form the permeate. In recent years NF has evolved to what today is called organic

solvent nanofiltration (OSN), an approach to perform separations in organic solvents at room temperature. In this membrane-based approach that operates in a range of 200-1000 Da, the solute is dissolved in an organic solvent and it's retained by the membrane (Patrizia Marchetti, 2014).

Organic solvent nanofiltration is mainly applied in the following processes:

- Concentration for solute enrichment and solute recovery
- Solvent Exchange
- Purification for impurities removal
- Catalytic processes, crystallization and chemical synthesis assisted process

All of the above applications are widely used in pharmaceuticals. For the special chemicals industry, the biggest usage of OSN is in catalytic processes, while with base and consumer chemicals the applications focused on concentration by solvent enrichment, recovery and impurity removal. The OSN solute enrichment technique applied to the pharmaceutical industry is mostly used for the isolation and concentration of antibiotics, pharmaceutical intermediates and peptide from organic solvents with examples such as the active pharmaceutical ingredient (API) recovery being applied in industrial processes. Another rise of solute enrichment via OSN but in the chemical consumers' industry was the increasing demand for natural and biological health products such as extractions of vitamins and antioxidants from herbs and plants. (Patrizia Marchetti, 2014) Another usage of OSN solvent recovery is in two-stage membrane cascade configurations, replacing liquid−liquid, liquid−solid and liquid−gas purification techniques that require large quantities of organic solvents and are prejudice for the environment (Patrizia Marchetti, 2014).

When it comes to API purification, the process accounts for around half of the costs in the pharmaceutical industry. A lot of studies show that OSN may be a solution for this purification phase, still, it has the problem of most of the impurities that should be removed tend to attack the polymeric membrane due to their reactivity. Adding to that, another limitation that comes with API purification using OSN is its low rejection and low yield of the product. (Patrizia Marchetti, 2014) Due to that fact the majority of the purification studies were reported in a laboratory scale but not in industrial scale, another problem of scale/up is the fact that when the MW of the compounds to separate is similar, it is necessary to use more than one stage filtration. Usually, two-stage counter-current NF cascade is preferred. (Silva, 2012) The membrane cascade mode has been applied in the purification of saccharides instead of using the usual simulated moving bed

chromatography, and even though it was necessary to have more than two-stage configuration, an economic evaluation showed that the more stages the more competitive it was compared with the chromatography (Patrizia Marchetti, 2014).

2.1.2. Transport Phenomena in Nanofiltration Membranes

The performance of a nanofiltration membrane is described by the solution-diffusion model, which assumes that the solvent and the solute don't interact with each other. It also assumes that the solute permeation is driven by the gradient in chemical potential of the solute i, Eq *Equation 1*. (Mulder, ChII Materials and materials properties, 1996)

$$J_i = -L_i \frac{d\mu_i}{dx} = -L_i \frac{R\,T\,d\ln(\gamma i\,Ci) + \vartheta i\,dp}{dx}$$

Equation 1. Solute flux of the membrane

Where the chemical potential $d\mu_i$ is dependent on solute concentration C_i (mol/m^3) and on the pressure difference across the membrane dp. R is the gas constant (8.31 m^3·Pa·K^{-1}·mol^{-1}), T is the absolute temperature (K), γi is the activity coefficient and ϑi is the molar volume (m^3/mol). Considering that the solution is diluted and applying Fick's law, *Equation 2*, becomes simplified

$$J_i = P_i\,\Delta C_i$$

Equation 2. Solute flux of the membrane

Where P_i and ΔC_i are the permeability and the concentration difference across the membrane of the solute respectively. Applying the same considerations for the solvent, the solvent flux is described as

$$J_v = \frac{(\text{Driving Force})}{(Total\ Resistance)} = \frac{\Delta \text{Peff}}{\eta_W * R_{tot}}$$

Equation 3. Solvent flux of the membrane

Which in this case depends on the effective pressure difference across the membrane, Δp_{eff}, *Equation 4* .

$$\Delta p_{eff} = \Delta p + \Delta \Pi$$

Equation 4. Effective Pressure of a membrane

This membrane difference is related to the osmotic pressure difference ΔΠ of the solutes at the two sides of the membrane. The selective transport through the membrane causes

a concentration increase of the less permeable solute near the boundary layer, this phenomenon known as concentration polarization is illustrated in Figure 2.

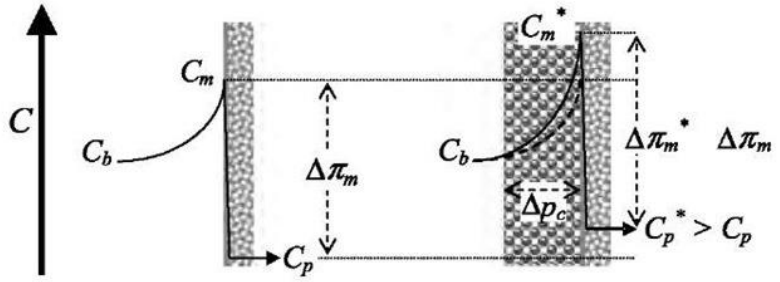

Figure 2. Concentration polarization phenomenon in nanofiltration. (Nanofiltration Separations Part 2 (Nanotechnology), 2019)

The increase in osmotic pressure leads to a decrease in the pressure, effective driving force. Nevertheless, the decrease in flux can also be caused by increasing of total resistance, *Equation 5*, which usually it's due to the concentration polarization or fouling. (Patrizia Marchetti, 2014)

$$R_{tot} = R_f + R_m$$ Equation 5. Total Resistance

Where R_f is the resistance caused by foulants and R_m is the resistance due to the membrane alone. The foulants resistance, R_f, is the resistance caused when a particle is entrapped in a pore, when the solubility limits of inorganic material are exceeded and they tend to deposit in the membrane causing the formation of a cake, or even when the solutes have chemical affinity and tend to interact with the membrane material causing adsorption of solutes to the pores walls. The foulants resistance can be reduced by chemical cleaning of the membrane. The resistance of the membrane, R_m, also known as the hydraulic resistance, is an intrinsic property of the membrane that reflects the pore structure and the interaction of the membrane and passage of the solvent in the same. This resistance has almost no impact in the total resistance. (A.Piry, 2012)

In order to select the best membrane to perform the fragment condensation synthesis, it's necessary to compare the different membranes at different conditions. The conventional procedure to compare membranes it's by analysing the filtration performance and to calculate the membrane effective rejection, R_{eff}. Solute rejection is an intrinsic property of the membrane related to the permeate concentration defined by *Equation 6*.

$$Reff\ (\%) = (1 - \frac{Cp,i}{Cm,i}) * 100$$ Equation 6. Effective rejection of a membrane

Where $C_{p,i}$ is the concentration permeate side and $C_{,mi}$ is the concentration in the retentate side near the membrane. There is no accurate method to measure the concentration of the retentate $C_{m,i}$, therefore it is necessary to introduce the concept of observed rejection, R_{obs}, which is inversely proportional to the measurable bulk concentration $C_{b,I}$, *Equation 7*.

$$Robs\ (\%) = (1 - \frac{Cp,i}{Cb,i}) * 100$$ Equation 7. Observed rejection of a membrane

Where $C_{p,i}$ is the concentration at permeate side and $C_{b,i}$ is the concentration in the feed bulk. This bulk concentration, $C_{b,i}$, is smaller than the concentration near the membrane, $C_{,mi}$, due to the concentration polarization.

As can be seen from the above reducing the concentration polarization resistance is of major importance to the membrane process. This could be achieved via intensifying the mass transfer within the membrane devise. Typically, at a large scale applications this is achieved via high recirculation rate provided by a pump. At a laboratory scale membrane devises sometimes mixing is provided via agitators. In order to understand the effects of mass transfer it is necessary to calculate some dimensionless number for agitation that determine the mass transfer performance. The data used are presented in Table 1.

Table 1. Dimensionless Numbers in agitation

Number	Symbol	Definition
Pumping	N_Q	Related to impeller capacities
Reynolds	N_{Re}	Laminar flow if Re<2000; turbulent flow if Re>4000
Power	N_p	Correlates Reynolds number with power requirements

Reynolds number for fluids in pipes is given by Equation 8, while in the case of the shaft power required to drive an agitator the Reynolds number is given by Equation 9, which can also be referred as impeller number due to the fact that is based on the impeller agitation. Depending on the agitation there can be three different types of flow

regions, laminar (Reynolds< 2000), transactional and turbulent (Reynolds> 4000). In an agitated tank, once a vortex starts to form near the impeller or stirrer it is a sign of a transitional regime. When this vortex begins to be at the surface the Reynolds number is usually above 4000 and the power is only dependent on the geometry of impeller hence the region is turbulent (Sinnott, R. K., 2005).

$$Re = \frac{D\ u\ \rho}{\mu}$$

Equation 8. Reynolds Number for fluids in pipes

$$Re = \frac{D^2\ N\ \rho}{\mu}$$

Equation 9. Reynolds Number for agitation speed

$$N_p = \frac{P}{\rho\ N^3\ D^5}$$

Equation 10. Power Number for impeller

Where

D: Diameter (m);

u: Superficial axial velocity (m/s);

ρ: Density (kg/m^3);

μ: Viscosity (kg/ m s);

N: agitator speed (s^{-1});

P: Power (W);

The power a stirrer/ impeller needs to mix a solution is given by the power number. This number is related to Reynolds by Figure 3.

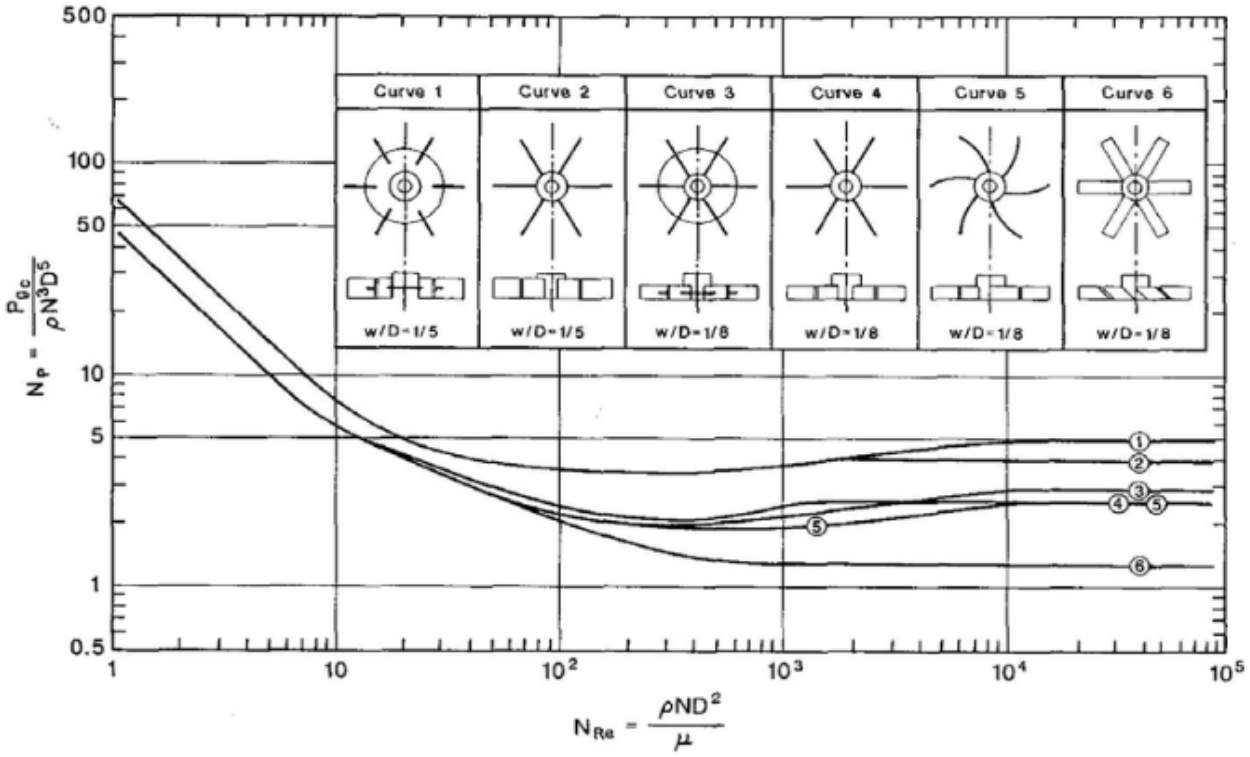

Figure 3. Power Number vs Reynolds Number (Sinnott, R. K., 2005).

This dependency is only effective for Reynolds below 10^3, above this value the power number is constant. As seen by Equation 10 the power number relates resistance with inertia forces. The efficiency of a stirrer/ impeller is given by the ration of power number and the pumping number, in which the smaller the ration the more efficient the impeller. (Chudacek, 1985)

2.1.3. Cascade and diafiltration modes

A cascade, is an array of separation units, also called modules, organized in stages, hence each cascade is composed of at least two separation units. There are ideal and non-ideal cascades. An ideal cascade design is obtained when the concentration of the recycled stream is equal to the retentate streams they are mixing. Even though ideal cascade designs are hard to achieve, usually the experimental procedures are approximated to an ideal cascade. (Ali K. Alshehri, 2015)

Regarding the modes, there are two main configurations of operating a cascade, the open-loop in which the permeate from the second stage goes to drain, and the closed-loop, in which the permeate of the second stage passes to the first stage, gradually diluting the content of the first stage. Considering that in most cases the rejection is not 100 %, the closed-loop cascade configuration modes require recycling of the solvent containing impurities, which means to recirculate this solvent back to the

separation stages. In this study the configuration is a countercurrent recycle closed-loop based on three basic sections:

- the feed stage;
- the stripping section, in which there is an increase in recovery of product, this section is below the feed;
- the enrichment section, in which there is an increase in product concentration, this section is above the feed.

The countercurrent two-cascade system has two major configurations, the stripping configuration and enriching configuration. The stripping configuration, is characterized by recycling of the permeate of the second stage to the first stage with the retentate of the first stage feeding the second stage. The enriching configuration is characterized by the opposite, with the permeate feeding the second stage and the retentate recycles to the first stage, Figure 4. One of the advantages of membrane cascade is that in this configuration the purification process is faster than with a single membrane without compromising of the yield or purity. (Ali K. Alshehri, 2015) Considering the enriching configuration with more than two stages, the concentration of the final product decreases from one stage to the other as the number of membranes increases, hence the number of stages in a cascade should be as small as possible. Increasing the number of stages also has the disadvantage of more complex process control. (Villani, 1979) (Benedict, 1981) In order to increase the recovery of the product, the configuration used in this work is a version of a countercurrent enriching cascade, Figure 4.

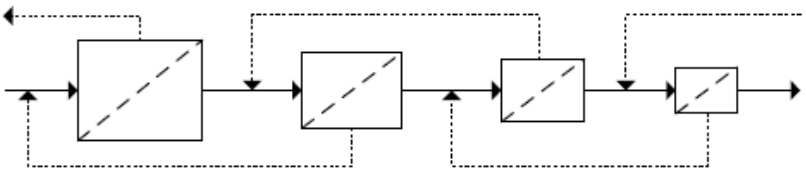

Figure 4. Countercurrent recycle cascade (Silva, 2012).

Regarding the diafiltration, it is a technique for the removal of permeable solutes from a solution in order to obtain high purity products. Diafiltration is a tangential flow filtration method in which there is addition of solvent to the pressurized side of the membrane and it consists of the following three basic phases:

- Concentration by passing the feed solution through membranes to obtain similar concentrations of low MW components in the retentate and the permeate;

- Addition of a diafiltration fresh solvent to purify the retentate bringing the volume to its initial value;
- Concentration of high MW solutes in retentate in the enriching stage. (ScienceDirect, 2019)

There are different modes of operation and configuration for the diafiltration to enhance mass transfer and to maximize energy efficiency. These modes are continuous also referred as constant volume diafiltration, Figure 5 A), and batch, Figure 5 B), which can be performed by sequential dilution or by volume reduction. The main difference between batch and continuous is on the solvent addition mode.

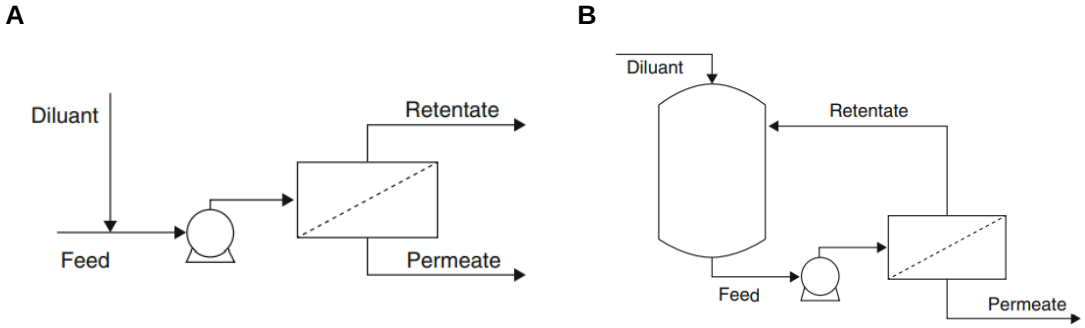

Figure 5. Flow diagram of Diafiltration configurations, (A) Continuous mode and (B) Batch mode (Kovács).

The continuous diafiltration the mode used in the present study, is based on the wash out of the lower MW solutes in the retentate by solvent addition at the same rate that the permeate leaves the system hence the volume of the system and the product concentration are constant. The continuous diafiltration process is more complex due to the fact that it requires a pump in order to add the solvent at a constant rate. This pump may also lead to a contamination of the product. Still one of its advantages is the fact that the concentration of the retentate is kept constant throughout the process (Fane, 2005) (Livingston, 2009) (Silva, 2012).

The batch diafiltration by sequential dilution is performed in cycles and the usage of solvent is smaller compared to the prior mode. In this case before the solvent addition, smaller solutes are removed while the concentration of retentate increases. Afterwards there is addition of fresh solvent and after this addition again the retentate is concentrated. In the case of batch diafiltration by volume reduction there is initially a concentration of the sample followed by a dilution to the original sample volume. For both batch modes, once the separation process is completed, the final product is obtained in the feed reservoir, and the final product has the same volume and concentration as the initial starting solution (Science Direct, 2019). In Table 2 is a summary for comparison of batch and continuous diafiltration modes in industrial-scale usage.

Table 2. Comparison of batch and continuous diafiltration (Kovács)

Characteristics/ Modes	Continuous	Batch
Control investment	High	Low
Feed volume flexibility	Low	High
Residence time	Low	High
Module efficiency	High	Low
Energy consumption	Low	High

2.1.4. Membrane cells

In membrane filtration, after the feed material is in contact with the membranes, the results are two streams, the permeate and the retentate. The permeate is the material that passes through the membrane's pore due to its smaller size. The retentate is the larger material that has a larger size than the pores and therefore is retained by the membrane. The separation unit of a membrane is called module and it can be flat or tubular. In this work the modules used are flat, Figure 6, with the pressure being applied in a parallel way to the membrane surface (Silva, 2012) (Vandezande, 2008).

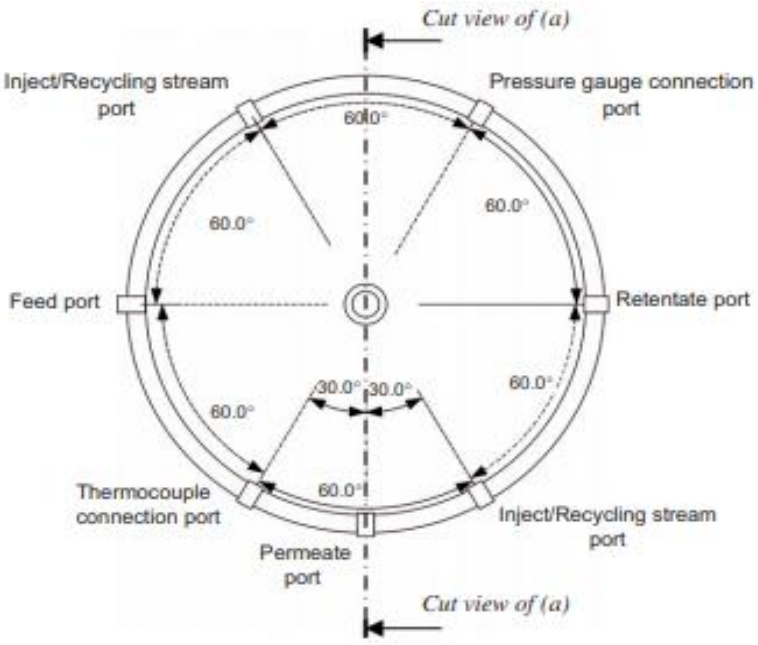

Figure 6. Schematics of the top view of the custom-made membrane cells used for the experimental set-ups of this work (Lin, 2007).

Comparing this mode to the dead-end flow mode, in which the feed and the permeate are flowing perpendicular to the sheet, the cross-flow is more efficient and used in industry, due to the fact that the parallel feed flow creates a gradient concentration on the membrane surface that consequently decreases the fouling tendency, polarization problems as well as cake formation (Silva, 2012) (Vandezande, 2008).

The first type of flat membranes cells to be used have the permeate coming from the top of the cover, Figure 7. These type of cells were also used in the second configuration for the diafiltration (Figure 22, Chapter 3.4.3).

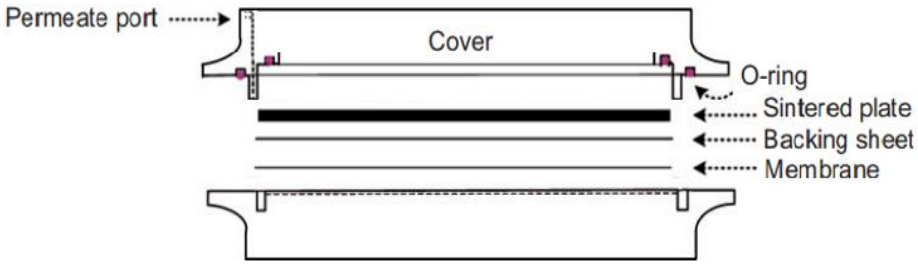

Figure 7. Schematics of the front view of the custom-made membrane cells used for the experimental set-ups used in single screening and diafiltration. Adapted from (Lin, 2007)

In the cascade (Figure 20, Chapter 3.4.2) and first configuration of diafiltration (Figure 21 Chapter 3.4.3) cells have a magnetic stirrer, Figure 8.

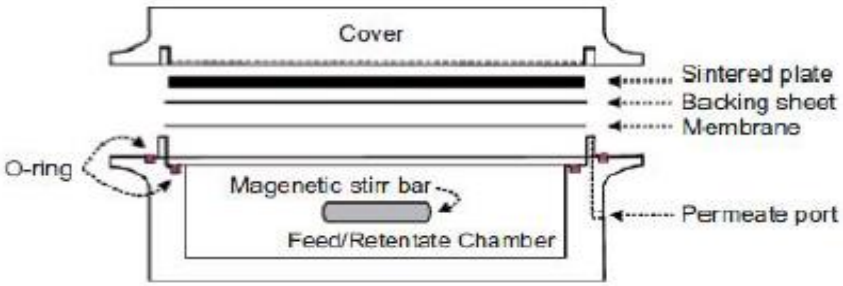

Figure 8. Schematics of the front of the custom-made membrane cells used for the experimental set-ups of this work. Adapted from (Lin, 2007)

2.2. Peptide Synthesis

Proteins are polypeptides, which are the assembling of up to 50 amino acids, linked to each other by peptide bonds. According to the IUPAC, when the ensemble of amino acids results in intermediate relative molecular weight peptide, it is denominated an oligomer.

Due to the importance of proteins and peptides in medicine, healthcare and biochemistry, one of the focuses of peptide research has to do with their synthetic production at a less costly price for the consumer. This works focuses on the study of the glucagon synthesis, which is a hormone that increases the blood sugar concentration preventing the body to achieve hypoglycaemia and it is used to treat diabetes type 2 (UK Gov, 2019).

There are currently twenty known natural amino acids for proteins building blocks, all of them with the same basic structure. Amino acids are chiral molecules and therefore have four groups attached to the central asymmetric α-carbon. The amino group (NH_2), called N-Terminus, and the carboxyl group (COOH) also called C-Terminus, represented on the right side, the hydrogen and the side chain group that confers different properties to the amino acids. Only L- enantiomers are used in cells and are incorporated in proteins, and therefore by convention, the amino group is always represented in the left side of the molecule while the carboxyl group is on the right (Termofischer Scientific, 2019).

The first peptide to be synthetized and also the simplest one was glycyl-glycine, by Fischer and Fourneau in 1901. Their technique is still in usage nowadays to produce semisynthetic peptides. It consisted of removal of the H_2O of the carboxyl group of one amino acid and afterwards joining this amino acid with the amino group of another amino acid. Initially, in order to avoid side reactions, all the groups were protected, prior to coupling, it was necessary to deprotect the amino group of the first amino acid and the carboxyl of the added amino acid, Figure 9. The stepwise principle (sequential addition of amino acids) with protection of all groups in both amino acids followed by deprotection of the amino-terminal group of the first amino acid and the carboxyl group of the second amino acid in order for these two sites to react, as well as, the removal of all protecting groups once the peptide sequence is complete, also called cleavage, are necessary steps in the current synthesis protocols.

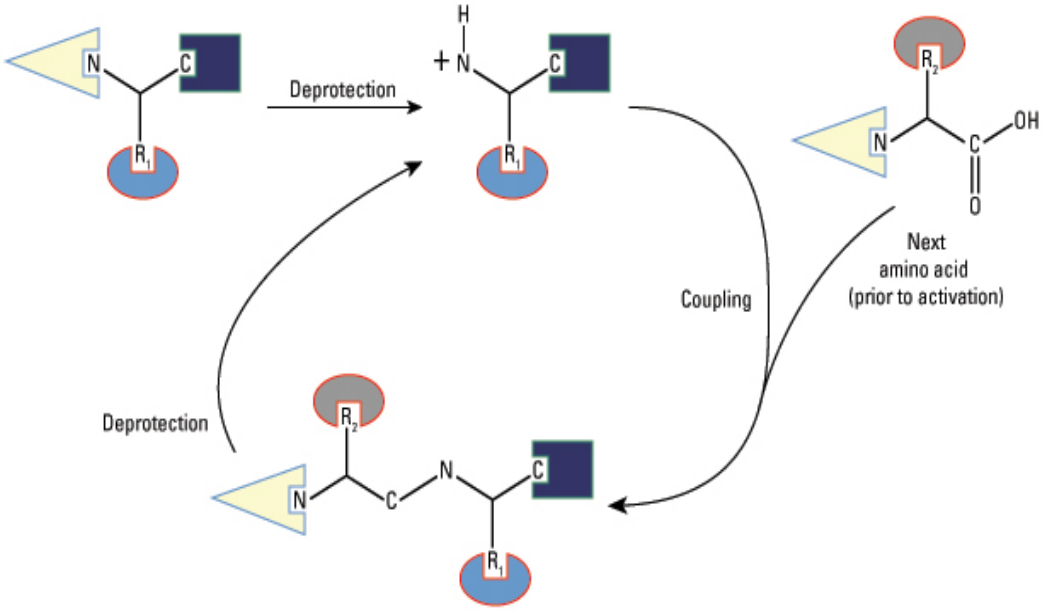

Figure 9. Schematic representation of the synthesis of a peptide. N, C and R represent the amino, carboxyl and side chain functional groups respectively (Termofischer Scientific, 2019).

Regarding the protection and deprotection of the different groups of amino acid, there are two main sets of conditions summarized in Table 3. Since the hydroxyl functional groups have similar reactivities, it is advantageous to use the orthogonal strategy allowing the efficient protection of several temporary protecting groups during the peptide synthesis.

Table 3. Protection and deprotection conditions (Termofischer Scientific, 2019).

Protection	Deprotection	Coupling	Cleavage	Wash
Boc/ Blz	TFA	Coupling agent in DMF	HF, HBr, TFMSA	DMF
Fmoc/ tBut	Piridine		TFA	

In case the amino acid N-terminal is temporary protected with tert-butoxycarbonyl (Boc), then the side chain needs to be permanently protected with benzyl (Bzl) (side chain functional groups are permanently protected throughout the reaction and are only removed once the reaction is completed), while the cleavage requires strong acids such as anhydrous hydrogen fluoride (HF) or trifluoromethanesulfonic acid (TFMSA). In the

case of HF, before its cleavage the Boc group must be removed with TFA/DCM to prevent t-butylation. Meanwhile, in order to reduce the risk of unwanted side reactions in the cleavage step, scavengers such as anisole, which are molecules that react with the cationic species released while removing the protecting groups, need to be added. After the scavengers' addition and the HF cleavage reagent has been evaporated, the synthetized peptide is obtained from the solution by washing with DMF. In the case of the cleavage with TFMSA, one of its advantages is that it does not require the removal of Boc group, but unlike HF, TFMSA is not volatile and therefore cannot be removed by evaporation. In this case the peptide must be precipitated from the solution using dry solvent ethyl ether. Due to the fact that peptide linkages can be affected by the acidic conditions the Boc strategy is usually not applied industrially unless basic medium conditions cannot be applied to the peptide (Bachem AG, 2016) (Termofischer Scientific, 2019) (Tarfah I.Al-Warhi, 2012).

In case the peptide can be synthesised in basic conditions, then the Fmoc strategy is preferred for the protection of the N-terminal. The base-labile protecting group 9-fluorenylmethoxycarbonyl (Fmoc) requires tert-butyl (tBu) for the side chain protecting groups and a base deprotection group such as piperidine in DMF. One of the problems occurring in Fmoc strategy is the Diketopiperadine (DKP) formation in side reactions, which is frequent when proline is one of the first two residues, which is not verified in glucagon sequence, Figure 10. The formation of aspartimide has also been reported in both acidic and basic medium synthesis with aminoacids' sequences such as Asp-Gly, Asp-Ala or Asp-Ser, which is also not verified for the glucagon, Figure 10 (Novabiochem, 2014) (Thermofisher Scientific, 1998).

His -Ser - Gln- Gly -Thr -Phe –Thr- Ser -Asp- Tyr- Ser- Lys - Tyr.- Leu- Asp -Ser –Arg- Arg- Ala- Gln- -Asp -Phe -Val - Trp -Leu -Met –Asn- Thr

Figure 10. Glucagon Peptide sequence

Regarding the protection of the carboxyl group of the first aminoacid, this is only required for the liquid-phase peptide synthesis due to the fact that with solid phase the resin/ solid support will serve as protecting group. Still, it is necessary to activate the C-terminal carboxylic acid of the remaining added aminoacids with dicyclohexylcarbodiimide (DCC) or diisopropylcarbodiimide (DIC) in order to react this site with the amine group of the forming peptide. DCC strategy is the most widely applicable due to the fact that can be used with the most common solvents know in peptide synthesis. Still one of the problems of both DCC and DIC it is the racemization.

To avoid this phenomenon it is necessary to add 1-hydroxybenzotriazole (HOBt) when synthesising in acidic medium (Boc strategy) and benzotriazol-1-yl-oxy-tris(dimethylamino)phosphonium hexafluorophosphate (BOP) or 2-(1H-benzotriazol-1-yl)-1,1,3,3-tetramethyluronium hexafluorophosphate (HBTU) for Fmoc strategy due to the fact that they require activating bases to mediate aminoacid coupling (Tarfah I.Al-Warhi, 2012).

Nowadays peptide synthesis can be performed either in solution/ liquid phase (LPPS) or in solid phase (SPPS). The first know approach, the solution phase, gave du Vigneaud, the Nobel Prize of Chemistry in 1955 for the synthesis of the first oligopeptide in solution phase (the hormone oxytocin). The solid-phase approach was only successfully applied years later by its pioneer Bruce Merrifield, who was laureate in 1984 with the Nobel Prize of Chemistry for his work in the SPPS approach. (Byrnes, 1994) These two approaches are described below.

In the solution-phase synthesis, the aggregation occurs in a solution phase and therefore, a C-terminal protecting group is needed on the first amino acid. In this synthesis, the Fmoc strategy is widely used due to the fact that Fmoc removing agent tris(2-aminoethyl)amine (TAEA) will form the dibenzofulvene, an adduct that can be extracted in phosphate buffer (pH 5.5). The Fmoc removing agent can also be 4-(aminomethyl) piperidine, with the disadvantage that may form precipitates or emulsions. The solubility of a protected fragment is not accurate, and therefore the coupling in a liquid-phase solution is difficult and it can take long periods of time, which makes this approach more appropriate for low molecular weight peptides.

The SPPS approach, schematized in Figure 11, is an approach for peptide synthesis based on assembly of amino acids on an insoluble polymeric resin bead functionalized with reactive groups that will link to the peptide chain. (Daniel Carbajo, 2019) The first step of the synthesis is assembling the carboxyl group of an amino acid to the resin, with this first amino acid being dependent on the resin used. Resins such as Rink amide resin, Pal resin, and Sieber resin are used in the Fmoc amides method. Whereas Wang resin, Sasrin resin, HMPB resin, trityl chloride resin, and 2-chlorotrityl chloride resin are used in the Boc acids method. (Wen Hou, 2017) Then, the N-terminal formed will attach to a new amino acid carboxyl group while the reactive groups are protected by a protecting group as explained previously. After each amino acid is added and the reaction is completed, the resin has to be washed with DCM or DCC. The synthesis in a polymeric support allows fast preparation of long peptides, still a restriction of the solid phase synthesis is the interaction of the amino acids with the resin and how it affects the coupling kinetics. To avoid these mass transference problems, it is required the use of excess reagents, that are removed by washing the resin in each coupling.

(U.S.A Patent No. US 9 260 474 B2, Method for solid phase synthesis of liraglutide, 2016)

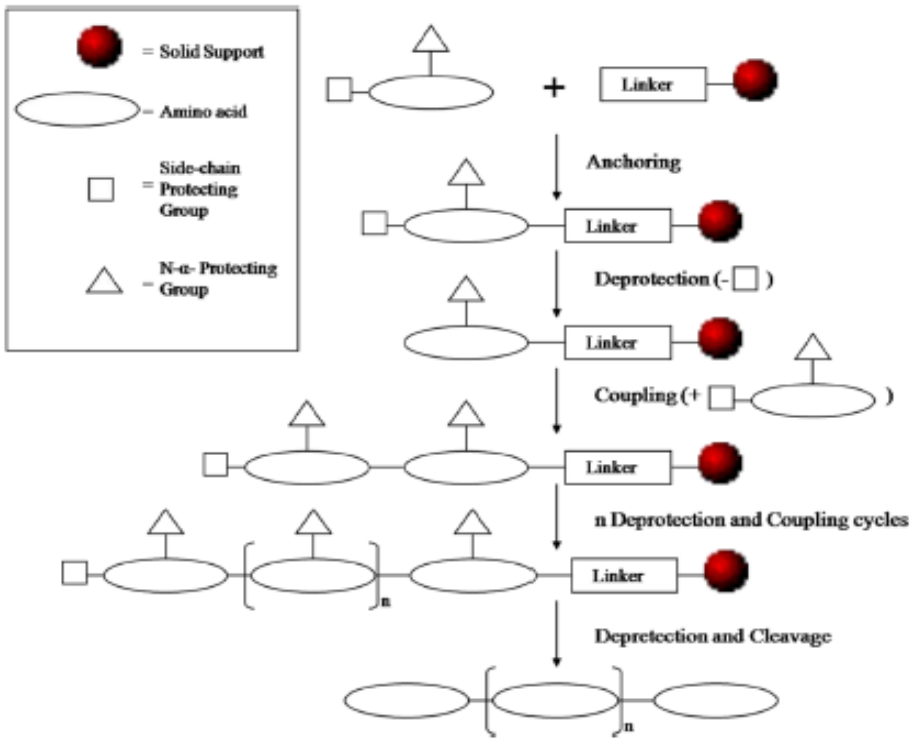

Figure 11. Representation of the stepwise solid phase synthesis, in which the peptide chain is built up from the C-terminal residue while bound to a polymeric resin support (Wen Hou, 2017)

During recent years, variations of these two approaches have been studied, including the usage of a PEG-linker, or also a Hub backbone, Figure 12, instead of a resin. The PEG linker is a molecule with the capacity of loading one peptide, while the Hub-1 is a soluble polyfunctional organic backbone molecule with higher peptide loading, three reactive alcohol groups. The Hub-backbone has the ability to covalently bind to a terminal of an initial monomeric unit. (Patent No. WO 2017/042583 Al, Defined monomer sequence polymers, 2017)

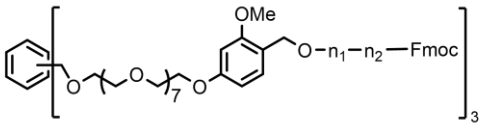

Figure 12. Hub-1 chemical molecular structure with fragments n1 and n2

After each coupling the excess unreacted reagents and by-products are separated from the growing polymer by diafiltration membrane processes. According to

the literature and using MATLAB simulations, when comparing single membrane and diafiltration processes in membrane cascade, diafiltration is more efficient due to the fact that the yield and purification of the product increase. (Patrizia Marchetti, 2014) Figure 13 is a schematic representation of peptide synthesis process with the PEG-linker as a support for the iterative coupling of aminoacids using the Fmoc strategy as the protection scheme. (Patent No. WO 2017/042583 Al, Defined monomer sequence polymers, 2017)

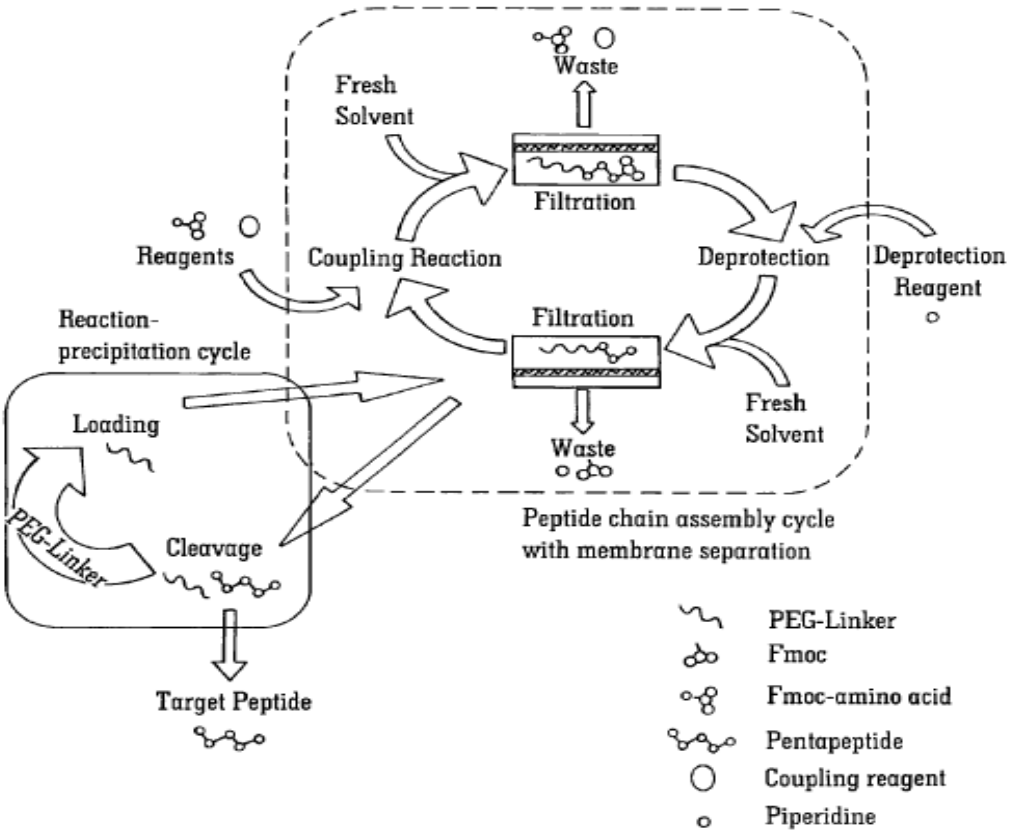

Figure 13. Schematic representation of a peptide synthesis via step-wise process with a PEG-linker (Patent No. WO 2017/042583 Al, Defined monomer sequence polymers, 2017)

Another approach, which is a variant of the sequential linkage of amino acids, is the fragment condensation approach. The fragment condensation can be both in solution or in solid phase using a support, Figure 14, and instead of iterative coupling of amino acids, the goal is to couple fragments (known sequence of amino acids that linked together form a peptide). The protecting schemes presented in Table 3 are also applied in the fragment condensation approach for the fragments protection.

A B

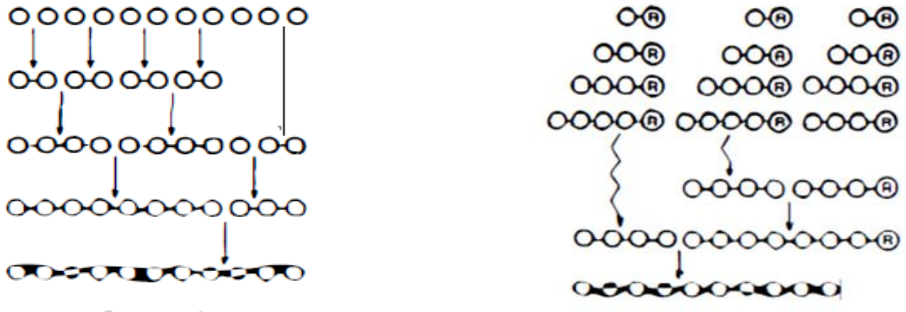

Figure 14. Strategies for the assembly of peptide Fragments. (A) Fragment condensation, carried out in solution phase; (B) Fragment condensation carried out in solid phase. The three different protected fragments are generated by stepwise solid phase synthesis, followed by released of two fragments from their original support and condensation on the new resin support that contains the first fragment. (Kent, 1988)

Taking in consideration the glucagon case study of this thesis, the fragment condensation is realized in liquid phase using the soluble Hub-backbone technology as the support for the fragments coupling and the Fmoc strategy as the protection scheme. The excess unreacted fragments are separated from the growing polymer by membrane processes, more precisely diafiltration cascade.

Table 4. Characteristics of the fragments

Fragment	MW (g/mol)	Fmoc off, Aniline on	Hub+ Fragments
1	1495	1347	5394
2	1635	1487	5769
3	2160	2012	7389
4	1597	1448	5700

The proposed 4 fragments have molecular weight between 1495 and 2160, Table 4 and after the Fmoc deprotection and C-terminal capping the MW of fragments will range from 1347 to 2012, Figure 15 and Figure 16.

HO——Asn(Trt)—Met—Leu—Trp(Boc)—Gln(Trt)—Val——Fmoc

Figure 15. Example of fragments from DG peptide

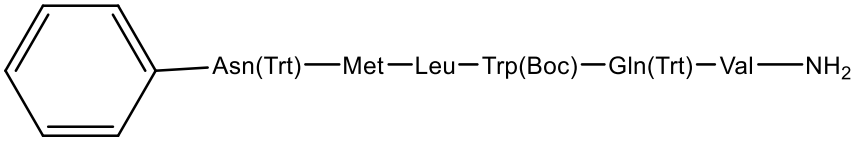

Figure 16. Example of fragments with Fmoc off, and aniline capping

Once the first coupling of a fragment to each alcohol occurs, the total MW of the molecule is about 8000Da, while the impurities and the by-products have around 2000Da. After the coupling of the second fragment, the total MW of the molecule is about 20000Da. (China Patent No. EP 3 196 206 A1, Method for preparation of liraglutide, 2017) (China Patent No. CN 104045705 A, Synthetic method of liraglutide, 2014) Taking in consideration the MW of the fragments, desired peptide, reagents and by-products, the solution tested was composed of poly(ethylene glycol) (PEG) oligomers with MW of 400, 1000, 2000, 8000 and 20000 Da in tetrahydrofuran (THF), which is an appropriate solvent for the diafiltration due to the fact that it maintains the functionalised polymer in solution.

3 . Materials and Methods

This chapter explores the materials and methods used in each experiment. Different types of membranes were used in this work, some of them were prepared previously by colleagues, Chapter 3.1, while other were prepared, Chapter 3.2.

3.1. Membranes studied but not prepared

The membranes not prepared but studied in this work, PEEK and PBI are categorized as Integrally Skinned Asymmetric (ISA) membranes. These membranes have ticker particles in the bottom than in the surface, hence the porosity, composition and structure vary across the membrane, Figure 17.

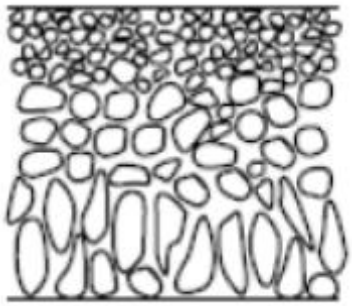

Figure 17. Schematic representation of ISA membranes. Adapted from (R.W., 2004) (Mulder, Ch I Introduction, 1996)

In these membranes the fluxes are higher than the usual due to the fact that the membrane is thinner and the microporous of the top has higher strength. (Baker, 2004) Both membranes were made by wet phase inversion technique, in which there is a phase inversion in the polymer from liquid to solid. Phase solidification is achieved with the following steps:

- Separation of the polymeric phase from the phase poor in polymer;
- Solidification of the polymeric liquid phase.

Even though the PBI and PEEK membranes were not prepared by me in the laboratory, the preparation process for these ISA membranes is described below and their structure is presented in Table 5.

Table 5. Chemical structure of of typical polymers used to prepare PEEK and PBI OSN membranes (Irina Boyanova Valtcheva, 2015)

Polymer	Chemical structure
Poly(ether-ether-ketone) (PEEK)	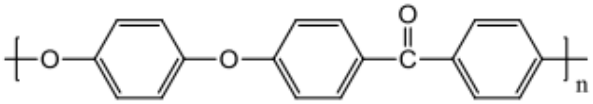
Polybenzimidazole (PBI)	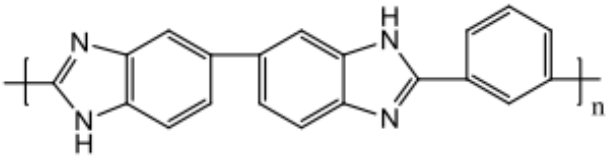

The PEEK membranes were prepared as follows: PEEK powder VESTAKEEP® 4000P was dissolved at a concentration of 12 wt. % in a mixture of 3:1 wt. % methanesulfonic acid (MSA) and sulphuric acid (SA) at room temperature until the polymer solution was homogeneous. Prior to casting the polymer solution was left to dry for 72-96 hours at 50 °C for PEEK_50ºC, and at 80 °C for PEEK_80ºC. (João da Silva Burgal L. P., 2016)

The PBI18m5j2005 membrane was prepared has follows: Celazole® S26 was diluted in N,N-Dimethylacetamide (DMAc) to 18 wt% polymer concentration until the solution was homogeneous. Prior to casting on non-woven polypropylene, the membranes were left to dry. Afterwards, the membranes were immersed in water at room temperature for 24h. Once the 24h were completed, the membranes were washed with IPA in order to perform crosslinking by immersion in a solution containing 3 wt% DBX in acetonitrile. After crosslinking, the membranes were immersed for 4 h in a solution of PEG400/IPA (1:1) solution. The IPA will remove residual reagents and the PEG400 will preserve the pore structure and allow dry storage. This membrane was also modified with j2005 polymer brush. The PBI18j1000 was prepared the same way PBI18m5j2005 with the difference that this time it was modified with a J1000 polymer brush (Irina Boyanova Valtcheva, 2015).

The summary of the membranes prepared by colleagues is presented in Table 6, as well as the filtration effective area of the discs for the single screening.

Table 6. Characteristics of the membranes used previously prepared by colleagues

Membrane code	Description	Membrane disc Area (cm^2)
PBI18m5j2005	PBI 18 wt%, Cross-linked with DBX, modified with J2005 polymer brush	52
PBI18j1000	PBI 18 wt%, Cross-linked with DBX, modified with J1000 polymer brush	52
PEEK 50ºC	PEEK support powder VESTAKEEP® 4000P 12 wt% in a mixture of 3:1 wt% MSA: SA, dried at 50ºC	14
PEEK 80ºC	PEEK support powder VESTAKEEP® 4000P 12 wt% in a mixture of 3:1 wt% MSA: SA, dried at 80ºC	14

3.2. Membranes prepared

The membrane prepared in the lab is a UF membrane with polydopamine coating, Figure 18. This coating is based on the same coating used by Jiang et al. with dopamine hydrochloride. (J.H. Jiang, 2011)

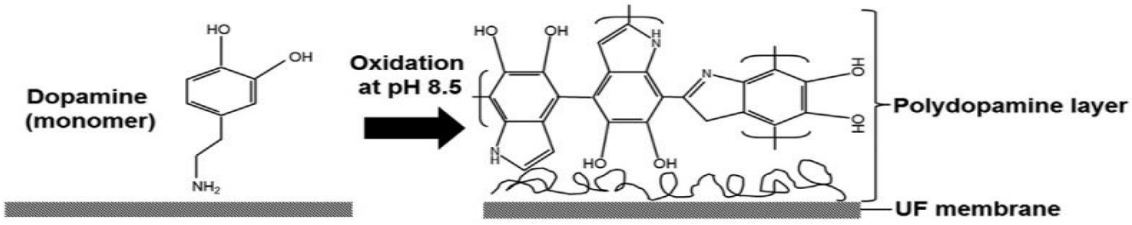

Figure 18. Self- Polymerization process of the dopamine monomer on the UF membrane (Kyoung-Yeol Kim, 2014)

The two catechol groups allow reactions with amine and thiol groups creating a quinone molecule with strong adhesion to solid surfaces. (Tomé, 2016) In order for the oxidation (oxygen present in the air) of dopamine to take place, it is necessary an alkaline solution. In case the PEG was in aqueous solution, if we tested the PE membrane and compared it when it has the polydopamine coating, it would be perceptible that because polydopamine coatings are characterized for enhancement of hydrophilicity, the flux of the PE membrane coated would be smaller than the PE membrane without coating. (McCloskey, 2010) (Tomé, 2016) In this polymerization process a mixing plate improves the oxidation strongly pH-dependent (Kyoung-Yeol Kim, 2014) (V. Ball, 2012).

3.2.1. Chemicals

PE sheets (SKL; BS) were purchased from SK Energy Co. Ltd. (Soul Republic of Korea). TRIZMA Hydrochloride (1M) and dopamine hydrochloride were purchased from Sigma-Aldrich (Germany) both used as additive. The NaOH (0.5 M) was used as a neutralizer.

3.2.2. Membrane Preparation

These membranes were prepared by dip-coating in alkaline conditions. Place space separators between 3 sets of PE sheets (SKL: BS) sheets. This set was placed in a 2L beaker filled with water and with a magnetic stirrer. For PDA 2gL, dissolve 10mM/L (3.15g/2L) TRIZMA hydrochloride in a beaker solution and afterwards dissolve 2g/L of dopamine hydrochloride. The formation of polydopamine particles is accompanied by a colorimetric solution change to dark brown. Once the solution presents a homogeneous brown colour, NaOH (0.5 M) was added until the pH reaches 8.5. (V. Ball, 2012) Each set of membranes was kept in solution for 18h, 30h and 40h. After the respective time, the PE sheets were taken from the beaker and washed with acetone at room temperature. Finally, the membrane was air dried for 1h at room temperature to remove the excess solvent. The PE membranes prepared for this work are listed in Table 7. For the PDA 4g/L the only difference from the previous preparation is that the concentration of TRIZMA hydrochloride and dopamine hydrochloride doubled to 20mM/L and 4g/L respectively. There is no specific rule regarding the order of applying the TRIZMA hydrochloride and the dopamine hydrochloride, because the reaction of polydopamine adhering to solid surfaces only starts once both reagents are in the solution.

Table 7. Summary of the PE membranes prepared

Membrane Code	Description	MWCO
PDA2gL_18h	PE coated with 2g/L of PDA for 18 h	N/A
PDA2gL_30h	PE coated with 2g/L of PDA for 30 h	N/A
PDA2gL_48h	PE coated with 2g/L of PDA for 48 h	N/A
PDA4gL_30h	PE coated with 4g/L of PDA for 30 h	N/A
PDA4gL_48h	PE coated with 4g/L of PDA for 48 h	N/A

3.3. Solvents and Solutions

The PEG is a polymer of monomers of ethylene oxide which could be used for different applications. Its length defines its applications. By definition PEGs have MW minor than 20000 g/mol and usually the MW proceeds the PEG classification. Above 20000 g/mol the classification is polyethylene oxide (PEO) and the classification polyoxyethylene (POE) applies to any molecular weight. Below 200 g/mol the polymer is a viscous liquid, between 200-2000 g/mol it's a wax, and above 2000 g/mol it's an opaque white crystal. PEGs are produced by an exothermic polymerization of water and ethylene oxide. Due to the fact that PEG has low toxicity levels, it's biocompatible and biodegradable and is also metabolized by the liver and the kidneys, PEG is widely used in the pharmaceutical industry. PEG is inert and it's biologically safe and therefore its usage via oral, dermal and intravenous administration is approved by the FDA. In the present study the solution with PEG was used due to its similar MW and the MW of the fragments. The solution (1g/L) used in the single screening was composed of PEG400, PEG1000, PEG2000, PEG8000, PEG2000 in the ratio 1:1:1:1:1. The solution used in the cascade and diafiltration configurations was composed of PEG2000, PEG8000, PEG20000 in the ration 1.5:1:1. The Polyethyleneglycol ether (PEG, MW≈ 400 $gmol^{-1}$) and Polyethyleneglycol ether (PEG, MW≈ 20000 $gmol^{-1}$) were purchased from Merck. Polyethyleneglycol ether (PEG, MW≈ 2000 $gmol^{-1}$), Polyethylene glycol ether (PEG, MW≈ 8000 $gmol^{-1}$) were supplied by Sigma-Aldrich (Germany). Polyethyleneglycol ether (PEG, MW≈ 1000 $gmol^{-1}$) was supplied by Fluka Research Chemicals (Germany).

Tetrahydrofuran (THF) is a colourless low-viscosity liquid ether and the ability of oxygen atom to coordinate with a magnesium ion, makes THF a widely used solvent for Grignard reagents. Due to that fact, THF is also widely used in chemical synthesis hence it was used as a solvent for the PEG solution. THF was purchased from VWR Prolabo Chemicals.

3.4. Filtration Configurations

3.4.1. Single Membrane Filtration

This work starts with the study of different membranes in a single- module filtration process due to the fact that the simplest membrane process design is with a single membrane filtration. The cross-flow rig system used for single membrane screening is schematized in Figure 19. It is constituted by feed tank with the PEG solution and two single membrane cells that have permeate and retentate outputs. The membrane cells discs tested had a membrane sheet diameter of 52 cm^2 for the PBI membranes in the single screening and for the rest of the screening their diameter was 14 cm^2. The samples, named P1, P2 and R and analysed in the HPLC. The pressure on the system is provided by the Amersham Pharmacia Biotech P-900 HPLC pump that provides a feed flow rate of 50 mL/min. In every experiment, before each filtration the system was washed with pure THF in the set-up conditions to wash impurities and prevent contaminations. Samples of permeate and retentate were collected 2 in 2 h during the day. The system was left to run at night.

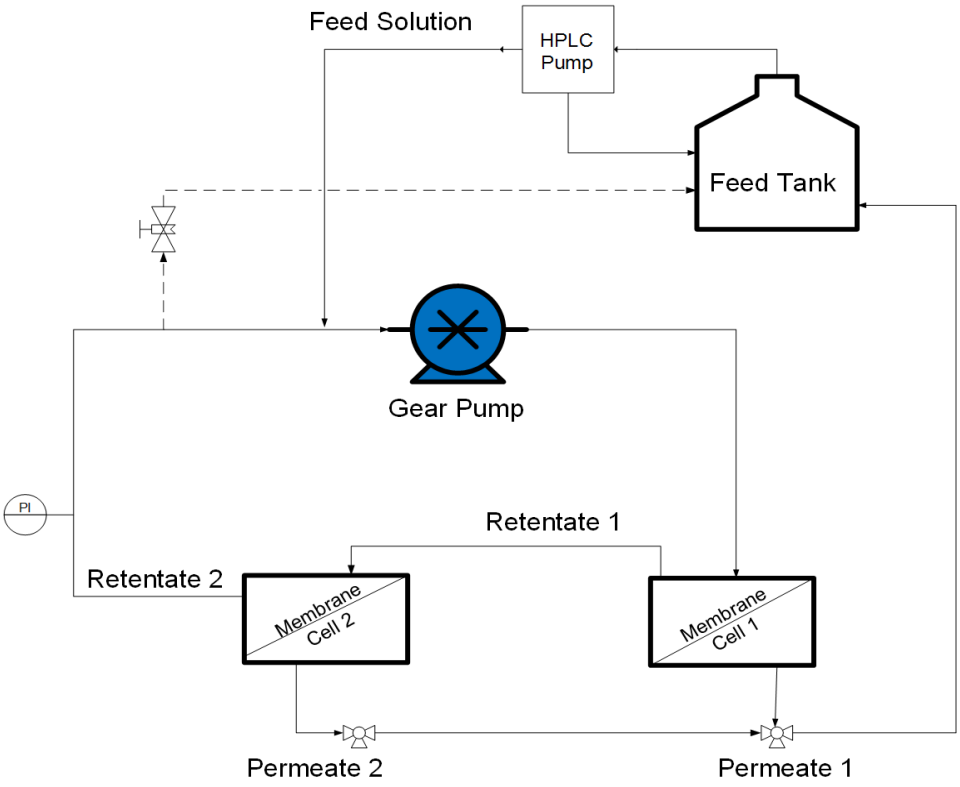

Figure 19. Schematic representation of the single stage organic nanofiltration membrane process integrating a cascade of 2 membrane units for purification.

The membranes tested and the pressures applied to the single system are presented in Table 8.

Table 8. Membrane code and pressure applied to the system

Membrane code	Pressure applied (bar)
PBIm5j2005	20
PBIj1000	20
PEEK50	5
PEEK50	10
PEEK50	20
PEEK80	5
PEEK80	10
PEEK80	20
PDA2gL_18h	5
PDA2gL_18h	10
PDA2gL_18h	15
PDA2gL_18h	5
PDA2gL_30h	5
PDA2gL_48h	5
PDA4gL_30h	5
PDA4gL_48h	5

3.4.2. Cascade configuration

In order to improve the performance of the membrane one can place several single modules in series. This configuration, Figure 20, is called recycling cascade and its phenome is based on the passage of permeate of the first membrane to the second membrane to be again separated in permeate and retentate. The retentate generated in the membranes is recirculated to the initial solution while the permeate of the last membrane is being constantly collected. The volume of each cell was about 30mL and the volume of the feed solution was 60mL. Therefore the total volume of the system, which corresponds to 1 vol, is 120mL with the first stage 90mL (feed tank and the first cell), while the second stage corresponds only to the second cell of 30mL This configuration operates in closed mode with permeate of the second stage being recirculated to the feed tank maintaining the feed tank volume constant. In this configuration the cells have a magnetic stirrer to maintain the homogeneity of the system. The HPLC pump had a flow rate of 50ml/min.

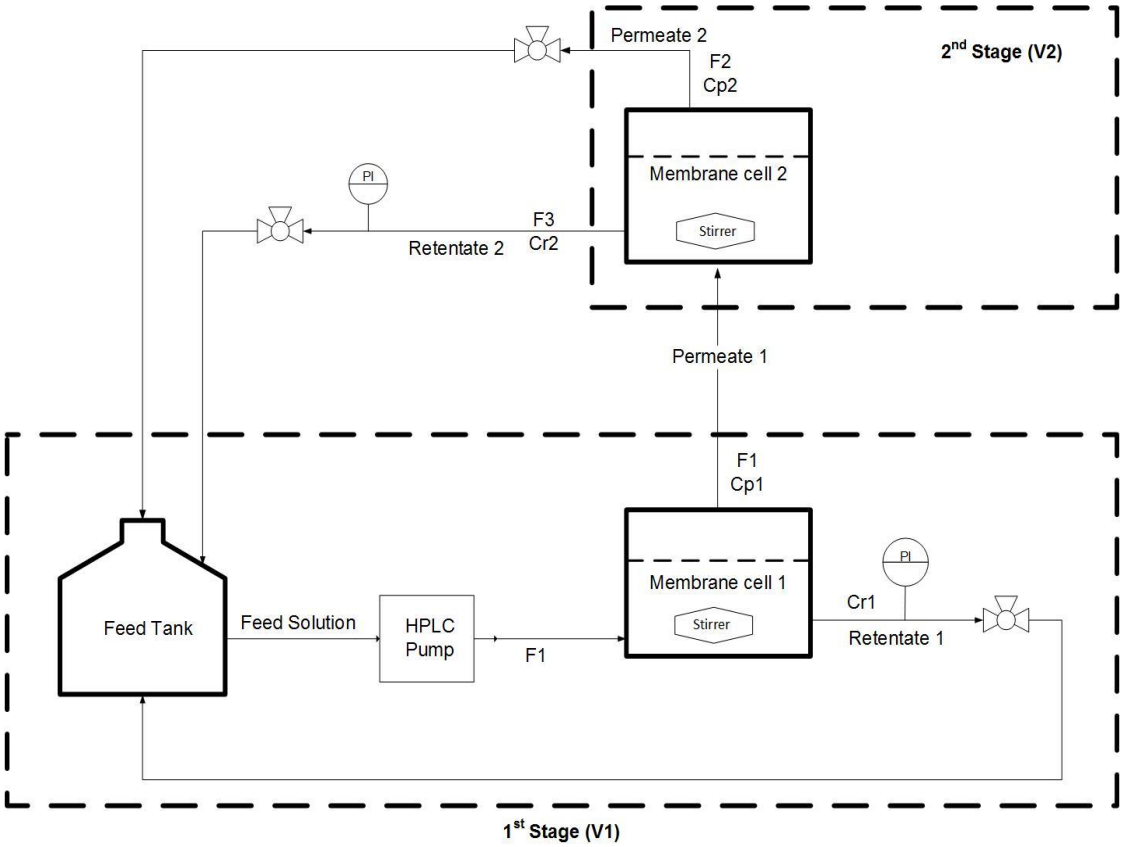

Figure 20. Schematic representation of the cascade membrane process integrating a cascade of 2 membrane units for purification.

3.4.3. Diafiltration configuration and modelling

To improve the separation of this pressure driven process and increase the yield and the purity, a diafiltration configuration can be applied, by constantly adding new solvent. The membrane diafiltration configuration, Figure 21, is similar to the cascade configuration, with the difference that in this case we introduce fresh solvent in the feed tank to maintain the volume of the system constant. This fresh solvent is introduced at the same rate that the permeate is being discharged in a vessel.

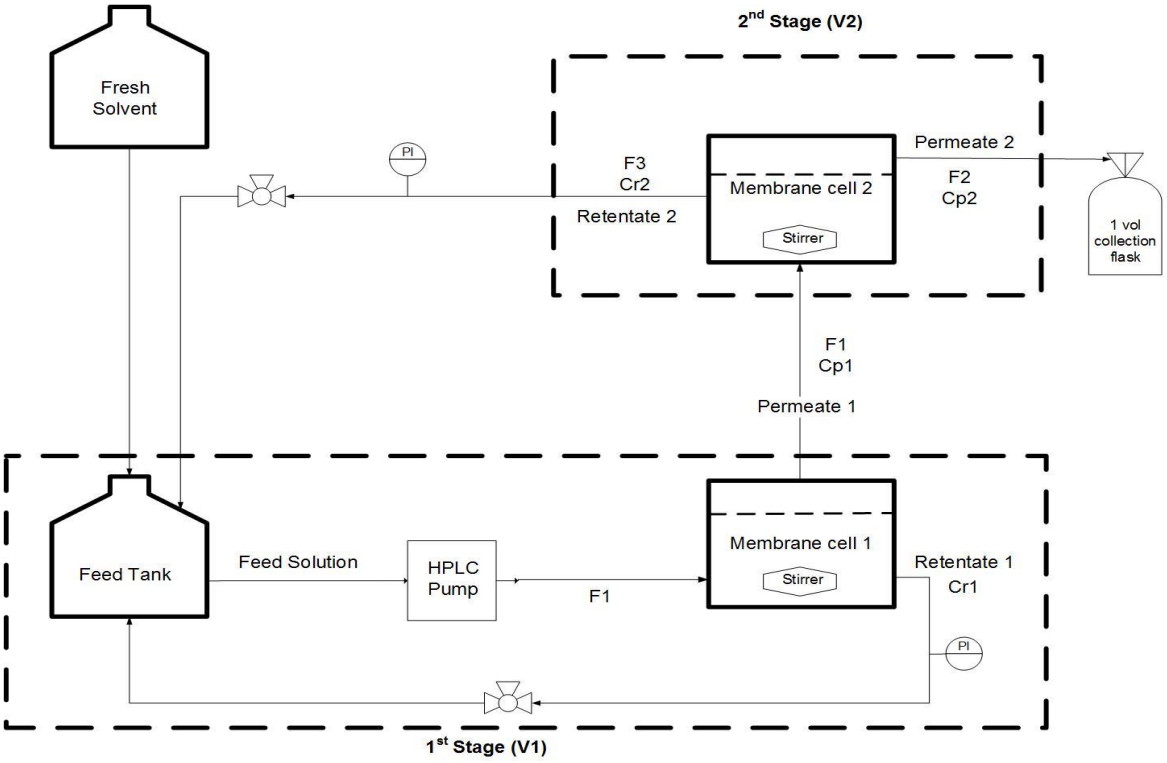

Figure 21. Schematic representation of the diafiltration membrane process integrating two membrane units for purification.

For the first configuration, Figure 21, the volume of each cell was about 30mL and the volume of the feed solution was 60mL. Therefore the total volume of the system, which corresponds to 1 vol, is 120mL, with the first stage 90mL, for the feed tank and the first cell while the second stage corresponds only to the second cell of 30mL. The HPLC pump had a flow rate of 50ml/min.

If the results obtained using the configuration above are not satisfactory a different configuration with pumps providing mixing in the system and enhancing mass transfer, can be used, Figure 22. In this case the total volume of the system equivalent

to 1 vol corresponds to 195 mL, 75mL from the feed tank, and 60mL each cell. The first stage corresponds to the fed tank and the first cell, 135mL, while the second stage is just the second cell, 60mL. The HPLC pump had a flow rate of 50ml/min.

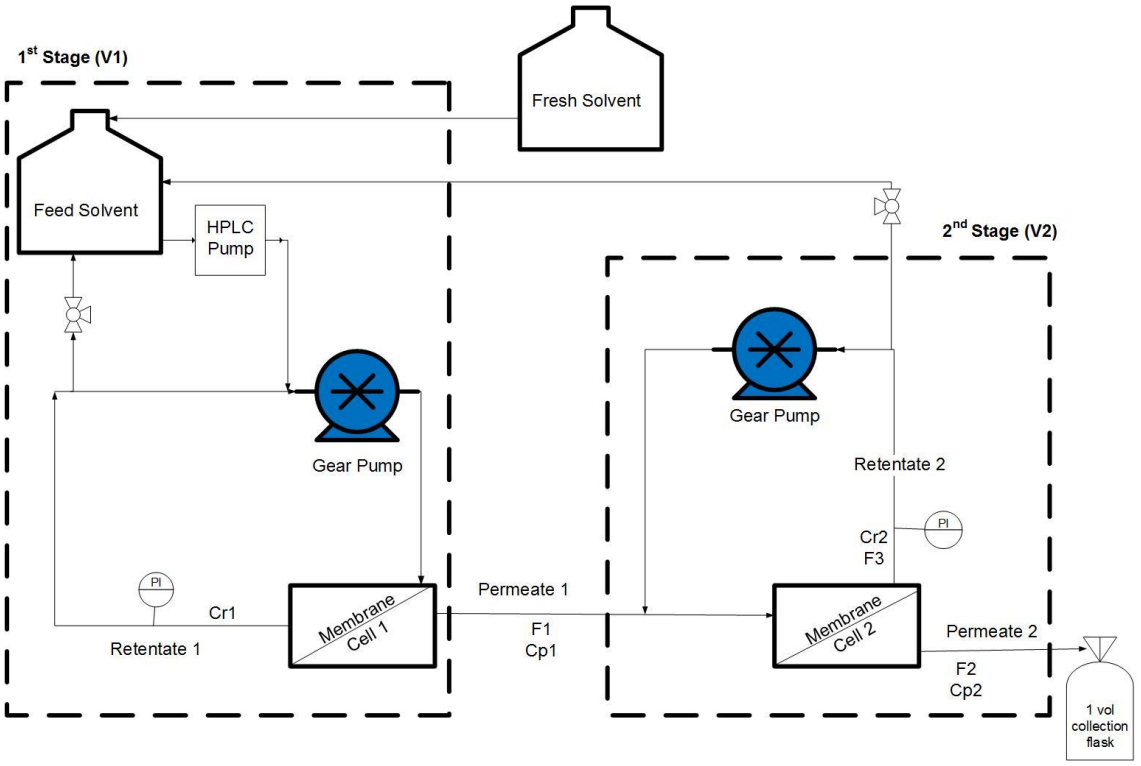

Figure 22. Schematic representation of the diafiltration membrane process integrating a cascade of two membrane units for purification.

In both configurations, only the feed solution of the first stage is rich in the component with highest rejection.

The simulations were carried out in MATLAB®, using the function ode45 and are an extension of a single stage membrane mass balance for both stages of the system to each component of the mixture that we pretend to separate, Equation 11. The model requires the variables permeance, rejection, the volumes of the tanks and the area, Annexe0. In the case of cascade simulation the variables were the experimental values obtained from the single screening for each membrane. Even though different scenarios were simulated, only the best four were tested experimentally. The variables for the diafiltration simulation were obtained from the four experimental cascade screening. The model assumes that the system is closed and no mass is lost and therefore the system operate at constant volume. The feed concentrations are 1.5 $g.L^{-1}$ for PEG2000 and 1 $g.L^{-1}$ for PEG8000 and PEG20000 and these components don't go under reactions once they are introduced in the cascade system.

$$V\ \frac{dC_{R,i}}{dt} = -F * C_{p,i} = J_v * A * C_{p,i}$$ Equation 11. Mass balance to diafiltration

By definition the observed rejection of species *i* is,

$$R_{obs} = 1 - \frac{C_{p,i}}{C_{R,i}}$$ Equation 12. Observed Rejection

And therefore the concentration profile for a single stage can be defined as

$$\frac{dC_{R,i}}{dt} = -\left(\frac{1}{V}\right) * J_v * A * C_{R,i} * (1 - R_{obs})$$ Equation 13. Concentration Profile

When the system is developed for the diafiltration two- stage membrane, the following four differential equations are be obtained, Equation 14, Equation 15, Equation 16 and Equation 17.

$$\frac{dC_{R1,i}}{dt} = \frac{1}{V_1} * [-F_1 * C_{R1,i} * (1 - R_{1,i}) + F_3 * C_{R2,i}]$$ Equation 14. Concentration gradient of stage 1 for species i

$$\frac{dC_{R2,i}}{dt} = \frac{1}{V_2} * [F_1 * C_{R1,i} * (1 - R_{1,i}) - F_2 * C_{R2,i} * (1 - R_{2,i}) - F_3 * C_{R2,i}]$$ Equation 15. Concentration gradient of stage 2 for species i

$$\frac{dC_{R1,j}}{dt} = \frac{1}{V_1} * [-F_1 * C_{R1,j} * (1 - R_{1,j}) + F_3 * C_{R2,j}]$$ Equation 16. Concentration gradient of stage 1 for species j

$$\frac{dC_{R2,j}}{dt} = \frac{1}{V_2} * [F_1 * C_{R1,j} * (1 - R_{1,j}) - F_2 * C_{R2,j} * (1 - R_{2,j}) - F_3 * C_{R2,j}]$$ Equation 17. Concentration gradient of stage 2 for species j

where *i* and *j* refer to the different species in solution to be separated. These equations will gives us four different columns of concentration. These four columns have *m* rows, depending on the time interval, defined as tspan.

F_2 and F_3 , Equation 18, depend on the recycle ratio, Equation 19, which is an independent variable that can be controlled depending on the flow we want for the permeate and for the retentate.

$F_1 = F_2 + F_3$ Equation 18. System flow rate balance

$$r_c = \frac{F_3}{F_1}$$ Equation 19. Recycle ratio

The yield and the purity profiles are obtained from the concentrations profiles of the differential equations. In the study case the product is the compound with highest rejection, the PEG8000 and PEG20000, hence the yield, Equation 20, and purity, Equation 21 are calculated considering the first stage only.

$$\mu_P(\%) = \frac{C_{R1,i} * V_1}{C_{Fi,0} * V_F} * 100$$ Equation 20. Yield of the product in the first stage

$$P_P(\%) = \frac{C_{R1,i}}{\sum C_{R1,i}} * 100$$ Equation 21. Purity of the product in the first stage

Where $C_{R1,i}$ is the concentration of component in the first stage, $C_{Fi,0}$ is the initial concentration of component in feed tank, V_1 is the volume of stage 1, while V_2 is the volume of stage 2 and V_F is the volume of the feed tank. The stage 1 is always the feed tank and the first cell while the second stage is only the second cell. The accuracy of the model created was proven using the conditions presented in the paper "When the membrane is not enough: A simplified membrane cascade using OSN" by Jeong F. Kim et al. Once the model was verified, it was also assumed that the fluxes and the rejections are constant throughout the operation and therefore the rejections and fluxes used were the average of the results.

3.5. Analytical method: High Performance Liquid Chromatography (HPLC)

In all the configurations rigs, the samples of permeate and retentate were analysed by Agilent 1100 Series HPLC system. Nowadays most of the High-Performance Liquid Chromatography (HPLC) separation columns work with an Evaporative Light Scattering Detector (ELSD) compared with Refractive Index (RI) detectors. The main goal of using an ELSD is that it detects samples that don't absorve UV light, like the PEGs. The principle of an ELSD is that the conversion of the eluents to a fine spray via a nebulizer, using nitrogen has the inert carrier gas. The ELSD analysis consists of the following three steps: nebulization, mobile-phase evaporation and detection. In the nebulisation, the nitrogen will flow through the effluent column in order

to form an aerosol. The nitrogen will afterwards be used in the mobile-phase evaporation which is heated allowing the evaporation of the mobile-phase. The final phase, the detection, is achieve by excitation of photons of the evaporated particles. (Dolan, 2003)

The reverse phase column (V14-8046, 250mmx4.6mm, ACE UltraCore 5 SuperC18) was used with the mobile phase A2 and B2 prepared in 2.5L flasks. Solvent A2 was a buffer of 0.97g of ammonium acetate in 2.5L of water (5mM) while solvent B2 was a solution of 80:20 of acetonitrile: methanol, respectively. The total flow was $1\frac{\text{ml}}{\text{min}}$, 10% A2 ($0.1\frac{\text{ml}}{\text{min}}$) and 90% B2 ($0.9\frac{\text{ml}}{\text{min}}$). In this chromatography the grade solvent used was acetonitrile (ACN), due to the fact that this solvent has lower absorvance, about 190 nm, which makes it the best choice for molecules that don't absorve UV light, like the PEGs. (Waters , 2019) For over 30 minutes, 30µl of elute collected sample were analysed and as a result, chromatograms like the one in Figure 23 were obtained. The identification of PEGs MW for each sample was based on the retention time (RT) of the PEGs' standard solutions (1g/L), Annexe. Table 9 presents the retention times of standard solutions.

Table 9. Retention Time of PEGs' Standard Solutions

Standard PEG solution	Retention Time (min)	Signal Area
PEG400	10.14	203.31
PEG1000	13.32	240.1
PEG2000	15.68	248.6
PEG8000	18.66	605.3
PEG20000	19.60	1204.2

It is possible to observe that the smaller the component analysed, the faster the elution, therefore the PEG400 signal is eluted first than PEG20000. In order to know the rejection it was assumed that the concentration ratio is proportional to the area ratio of the corresponding peaks.

From Figure 23 it is verified that lower MW PEG have shorter RT, which is expected since lower MW PEGs with longer non-polar chains tend to be less strongly adsorbed to the column.

A

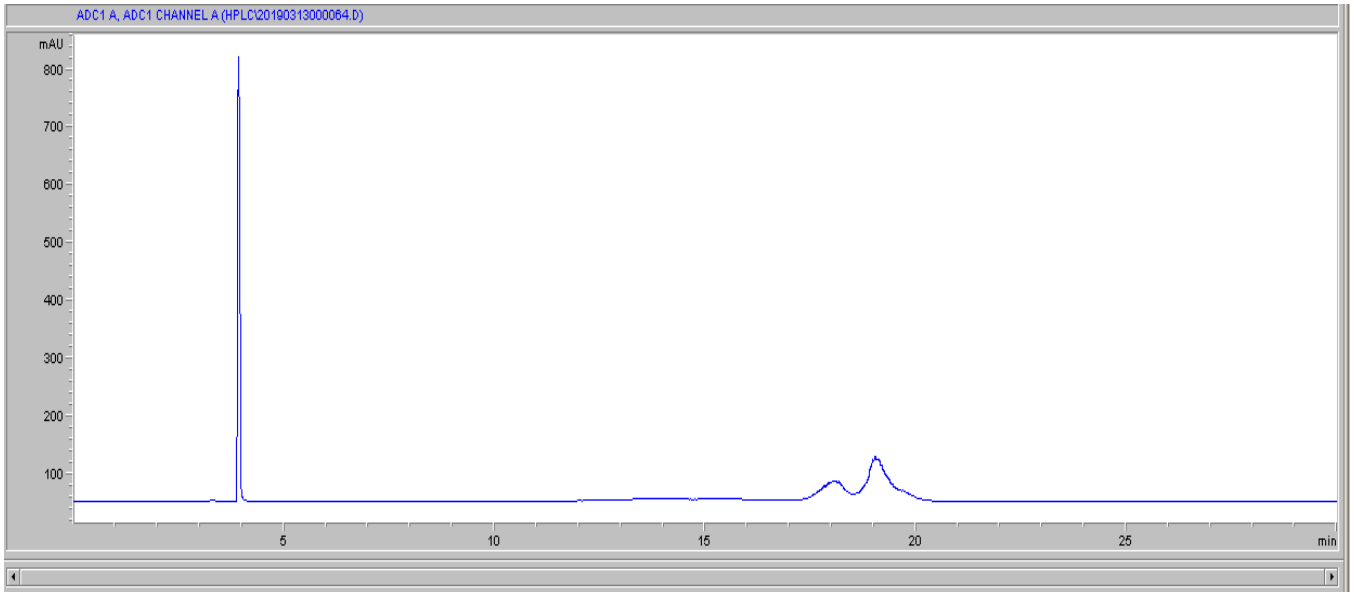

B

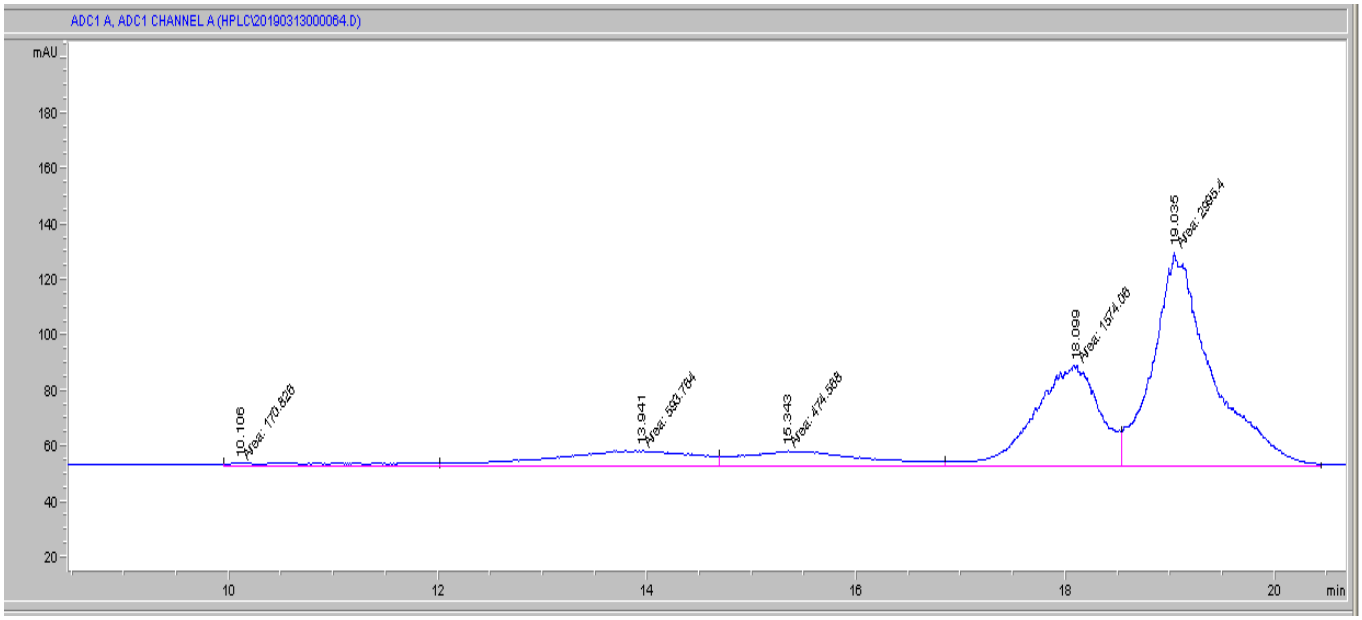

Figure 23. Example of an ELSD detector curve for PEG solution (400, 1000, 2000, 8000 and 20k DA) (1g/L) (A) without integration, (B) with area integration considering the RT presented in

3.5.1. HPLC calibration

To calculate the purity and the yield it was necessary to convert the HPLC peak areas to concentration and mass. For that it was necessary to calibrate the HPLC. A solution of 1g/L in 100mL of PEG2000, PEG8000, PEG20000 was prepared and then diluted in 16 solution in 20mL flasks, with concentrations (g/L) of 0.01, 0.02, 0.025, 0.05, 0.1, 0.15, 0.2, 0.25, 0.3, 0.4, 0.5, 0.6, 0.7, 0.8, 0.9, 1. The calibration curve is presented in Figure 24.

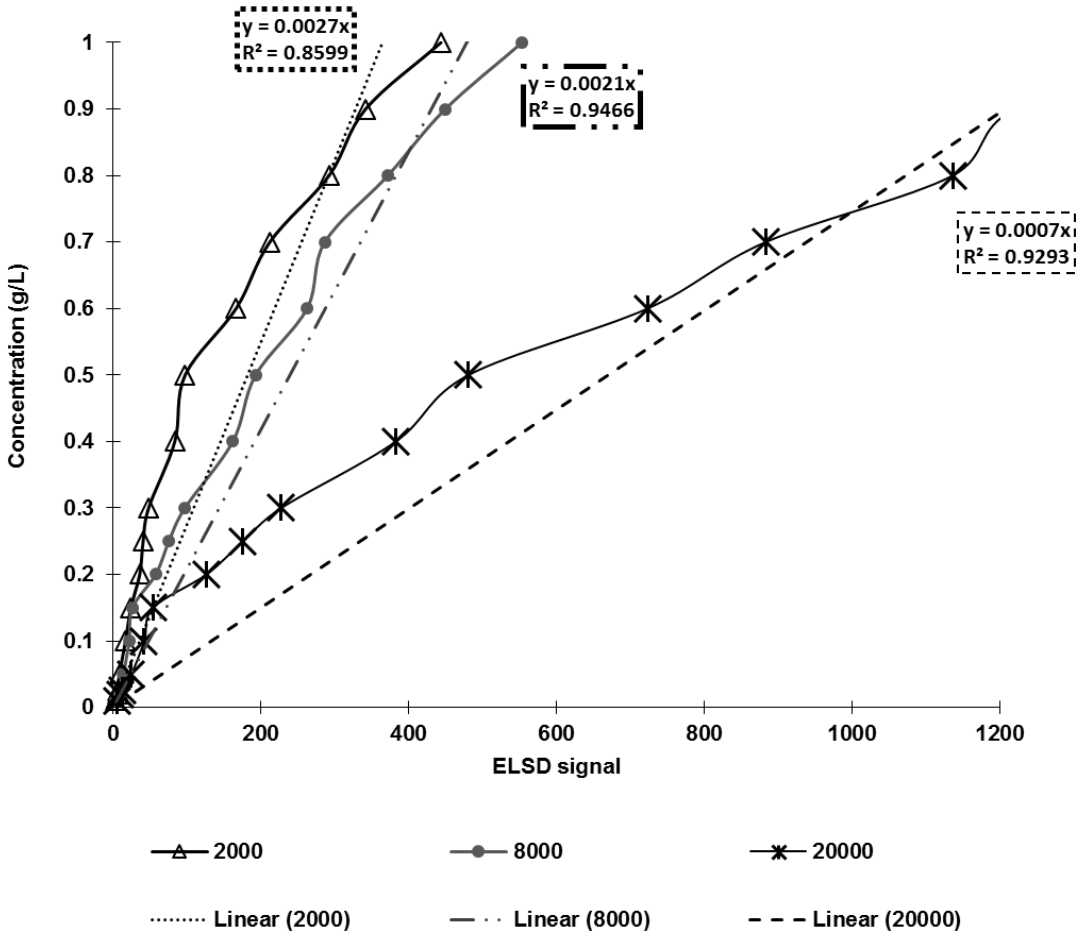

Figure 24. HPLC calibration curve.

3.6. Membrane Morphology- SEM

SEM images are a useful tool for the characterization of the membrane properties. One of the advantages of SEM is that it gives information about the functional performance of the membranes and allows their structural characterization. The cross-section was broken in liquid nitrogen and placed vertically in the stubs while the horizontal sample was simply cut at room temperature and placed horizontally on the stubs. Due to the fact that polymeric membranes are non-conducting, the samples of the membranes were coated with 15 nm of chromium using a sputter coater Q150T S (Quorum Technologies Ltd). A Field Emission Scanning Electron Microscope was used to acquire the high resolution SEM images with an accelerating voltage of 5 kV and under dry conditions at room temperature.

4 . Results and Discussion

4.1. Single membrane Screening

In order to select a membrane that is able to separate PEG2000 (MW= 2000 $g.mol^{-1}$) from larger PEGs. In order for this to happen, the OSN membrane needs a rejection close to 100% to intermediate oligomers with 8000Da and larger and the minimum rejection possible for oligomers of 2000Daand lower. Samples of permeate and retentate were taken and analysed in the HPLC and was compared with the standard samples (1g/L), Figure 23 B), Chapter 3.5.

The results presented in this chapter are average of the two membranes and permeates obtained during the single screening for PEG400, PEG1000, PEG2000, PEG8000 and PEG20000 using different membranes.

Figure 25 A) and B) it is possible to see that all the PEEK membranes have a rejection above 70% to all PEG MW, hence the membrane is too tight and even 400 Da molecules cannot pass through the membrane. The PEEK_80ºC have higher average rejection than PEEK_50ºC. PEG1000, PEG2000, PEG8000 and PEG20000 have similar rejections at 5 bar, 10 bar or 20bar. In all PEEK membranes the rejection for PEG1000 and larger intermediate oligomers is above 90%, therefore PEEK membranes cannot separate molecules with MW in the range 1000- 20000 Da. The experiments were not repeated, therefore the results are inaccurate, in order to decrease the error and have more accurate results the experiments should have been repeated.

A

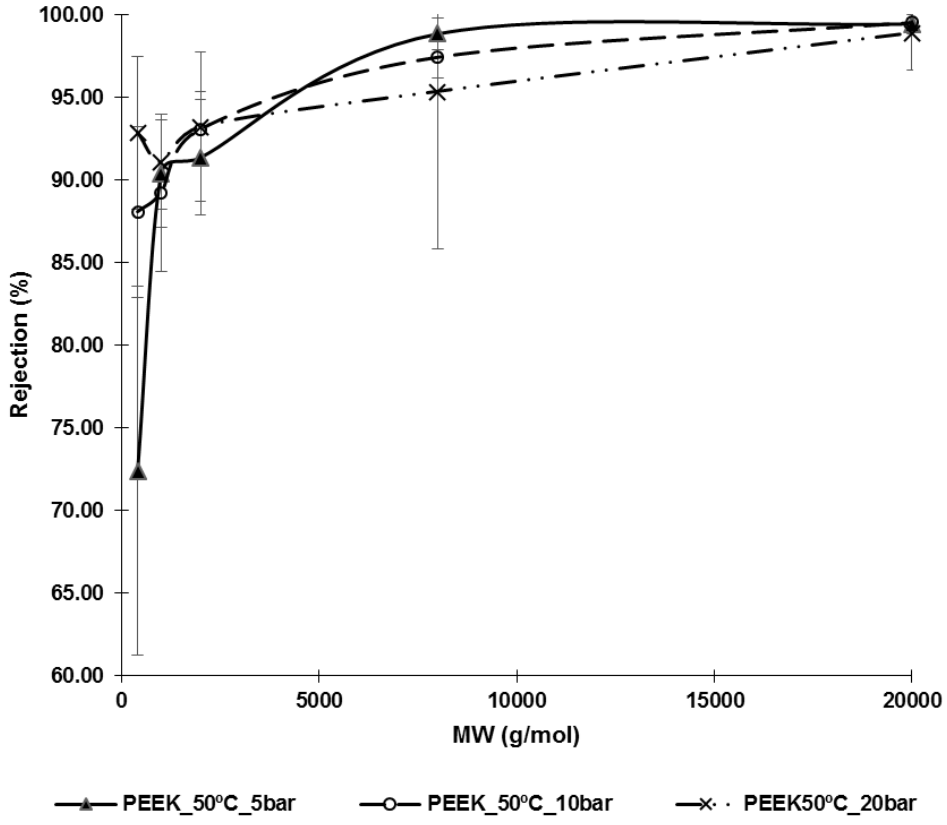

B

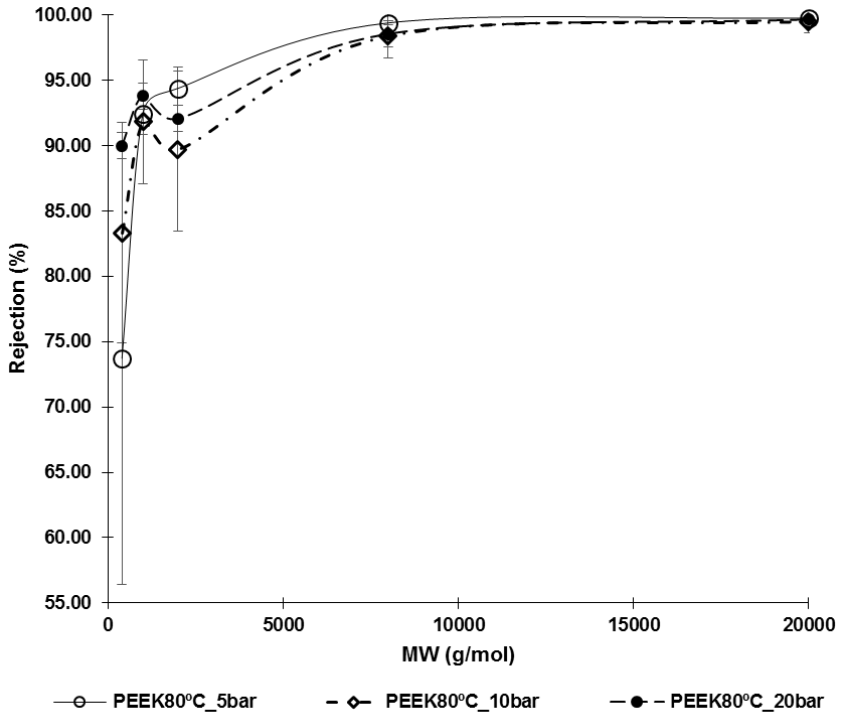

Figure 25. MWCO curve for A) PEEK_50ºC membranes in single screening and B) PEEK_80ºC membranes in single screening.

Due to the fact that PEEK membranes prove to not separate molecules with MW smaller than 2000 from molecules with MW large than 8000, these membranes were not used in the further studies with cascade and diafiltration configurations.

From Figure 26 B) and D) it is possible to see the different membrane composition typical of ISA membranes, Figure 17. In this case the toplayer (0.1- 0.5 μm of thickness) composed of smaller pores offers more resistance to mass transference than the sublayer composed of particles with larger pores (50-150 μm of thickness) that offer mechanical support to the toplayer. PEEK50ºC, Figure 26 A), is tighter than the PEEK80ºC, Figure 26 C), giving us the trend that the lower the temperatures in which the membrane were left to dry the tighter the pores. (Burgal, 2016) Another way of comparing pore size that doesn't involve SEM images is by measuring the permeability with pure solvent for a period of 24h and applying the same transmembrane pressure conditions to all the membranes. In most of the cases the membranes with higher permeability have bigger pores while the ones with smaller permeability have smaller pores.

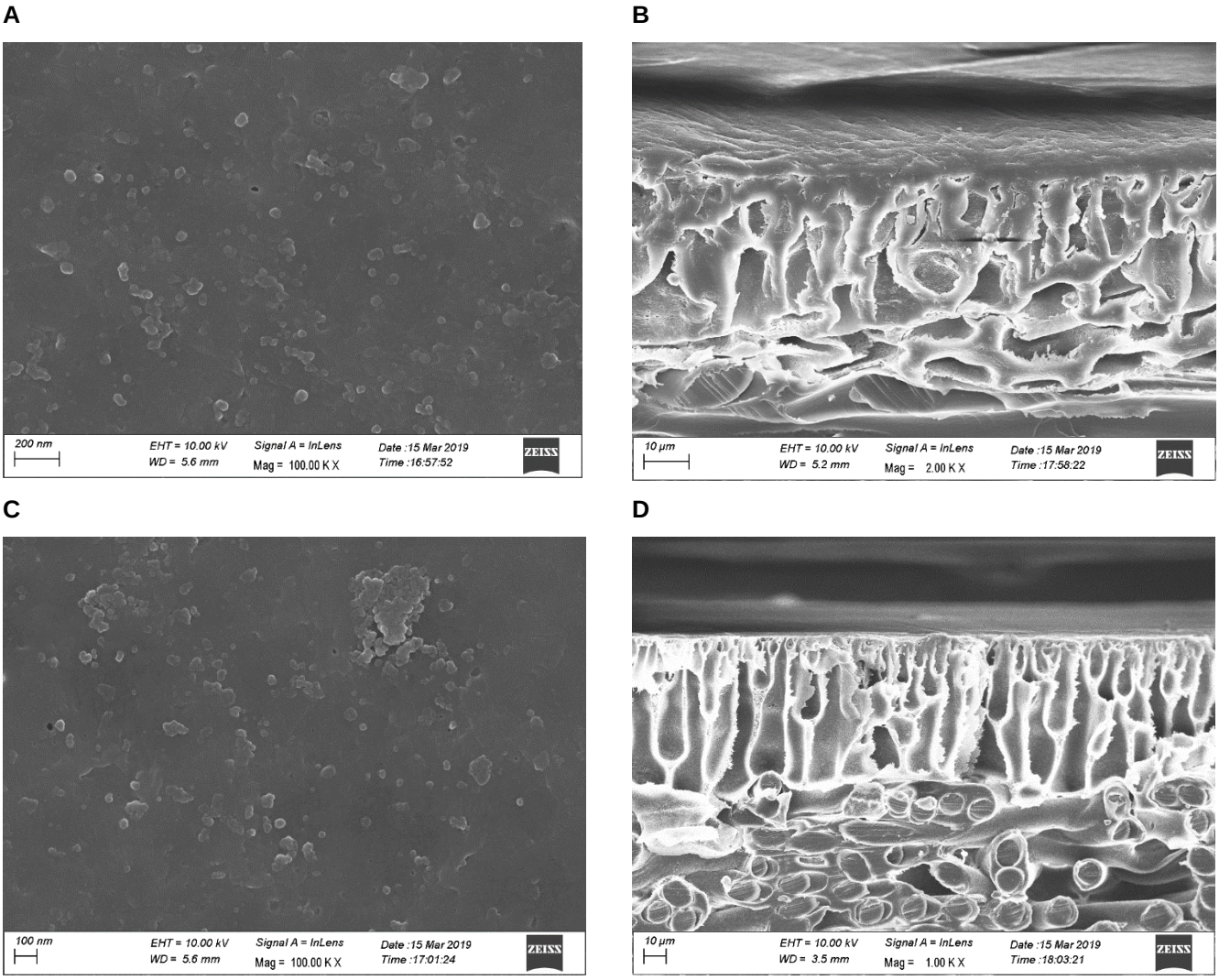

Figure 26. SEM image of membranes. (A) Top-section view of PEEK 50ºC at 100000x magnification; (B) Cross-section view of PEEK 50ºC at 1000x magnification; (C) Top-section view of PEEK 80ºC at 100000x magnification; (D) Cross-section view of PEEK 80ºC at 1000x magnification.

Regarding PBI, Figure 27, both membranes have less than 10% of average rejection for PEG400. Still in PBI18m5j2005 the PEG1000 and PEG2000 increase the rejection to about 82%. For this same membrane, PEG8000 and PEG20000 have a rejection of 97% and 99%, respectively. Therefore the PBI18m5j2005 membrane is not suitable for the separation of PEG1000 and PEG2000 from PEG8000 and PEG20000. In the case of PBI18j1000, the greatest difference from the former is that PEG400 as 6% rejection and for PEG1000 the average rejection is 51%. PEG2000 has a rejection of 78%, while PEG8000 and PEG20000 have better average rejection than the former PBI membrane, almost 100%. The negative rejection may be due to the HPLC calibration. The calibration curves were fitted as linear with a square error of the regression line between 86-95%. A polynomial curve, would fit the data better and therefore would have

diminished the errors of the regression line and could have avoided the negative values of rejection. For the same reason as mentioned before, the experience should be repeated in order to decrease the error and the experiment be considered reproducible.

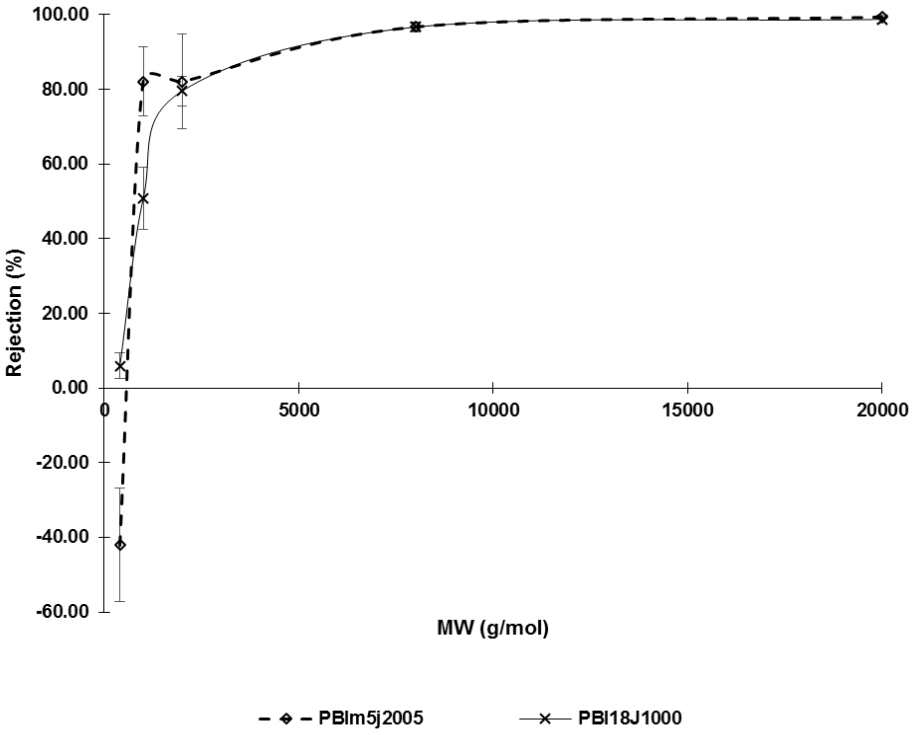

Figure 27. MWCO of PBI membranes in single screening.

Figure 28 presents the same data of PDA2gL_18h membrane and tested at different pressures to understand the effect of pressure in rejection.

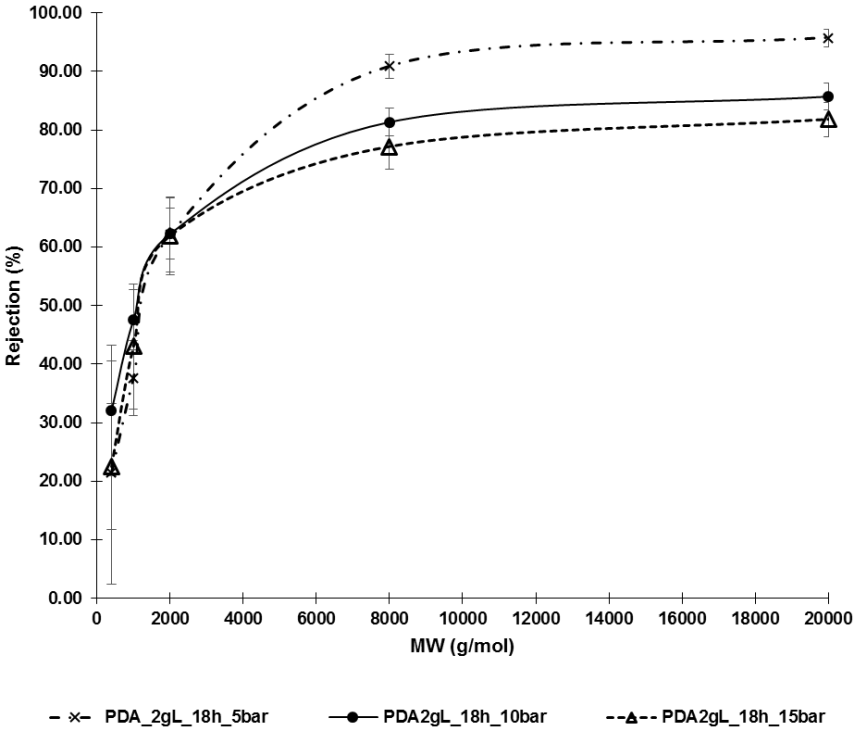

Figure 28. MWCO curve for the single screening of PDA membraes tested at different presures.

For the same MW at different pressures, the increase in pressure leads to a decrease in rejection for particles larger than 2000Da. Meaning that membrane tested at 15 bar achieves a maximum rejection of ~80%, while the one tested at 5 bar achieves a rejection of 96%. Considering that the goal is to have a rejection close to 100% for PEG 8000 and PEG20k, and the minimum for PEG2000 and smaller, lower pressure conditions are more adequate than higher. This phenomenon of increasing the pressure leads to a decrease in rejection is predicted by the gel polarization model. The model states that the increase in pressure leads to an increase in flux, which leads to an increase of convective transport of solutes through the membrane. When the concentration of solutes being transported increases, they start to accumulate near the surface, until the back diffusive mass transport equals the convective transport. This gradient concentration removes solute from the membrane, leading to a decrease of PEG8000 and PEG20k retention. (Zambujo Pé-Leve, 2012) (N.M. D'Souza, 2003) For MW smaller than 2000Da the PDA2gL membrane presents an irregular behaviour with rejection being independent from the pressure. The polydopamine didn't dissolve properly and the undissolved particles blocked the pores. Due to that, the PEG solution is more retained by the membrane with a coating of 18h and so the rejection is higher than when the membrane was coated for 48h. In the coating for 48h the polydopamine dissolved and therefore there was no obstruction of pores to the passage of solute and

more PEG2000 were able to cross the membrane, but also bigger PEGs where able to cross some of the membrane pores.

Figure 29 presents the data of the PDA2gL membrane prepared with the method of Chapter 3. In this case, the PDA 2gL_30h and PDA2gL48h have rejections for PEG2000 of 46.29% and 36.46% respectively. PEG8000 and PEG20000 have rejections in the range of 70-80%. While PDA 2gL_18h has rejection for PEG2000 of 69.61% and 87.27% and 88.62% for PEG8000 and PEG20000, respectively. According to the literature the membranes with higher coating time should be ticker, hence have higher rejection, but only PEG1000 has the expected behaviour, i.e., the more the time the PE membrane was in the solution with polydopamine the tighter membrane pores are and therefore the rejection increases from 18h to 30h and to 48h. Hence there isn't a verified trend between MW and rejection for MW below 2000Da. For PEG2000, PEG8000 and PEG20000 the opposite was verified with the average rejection decreasing with the increasing of time in the polydopamine solution. In 18h the polydopamine didn't dissolve properly and the undissolved particles blocked the pores, Figure 30. Due to that, the PEG solution is more retained by the membrane with a coating of 18h and so the rejection is higher than when the membrane was coated for 48h. In the coating for 48h the polydopamine dissolved and therefore there was no obstruction of pores to the passage of solute and more PEG2000 were able to cross the membrane, but also bigger PEGs where able to cross some of the membrane pores.

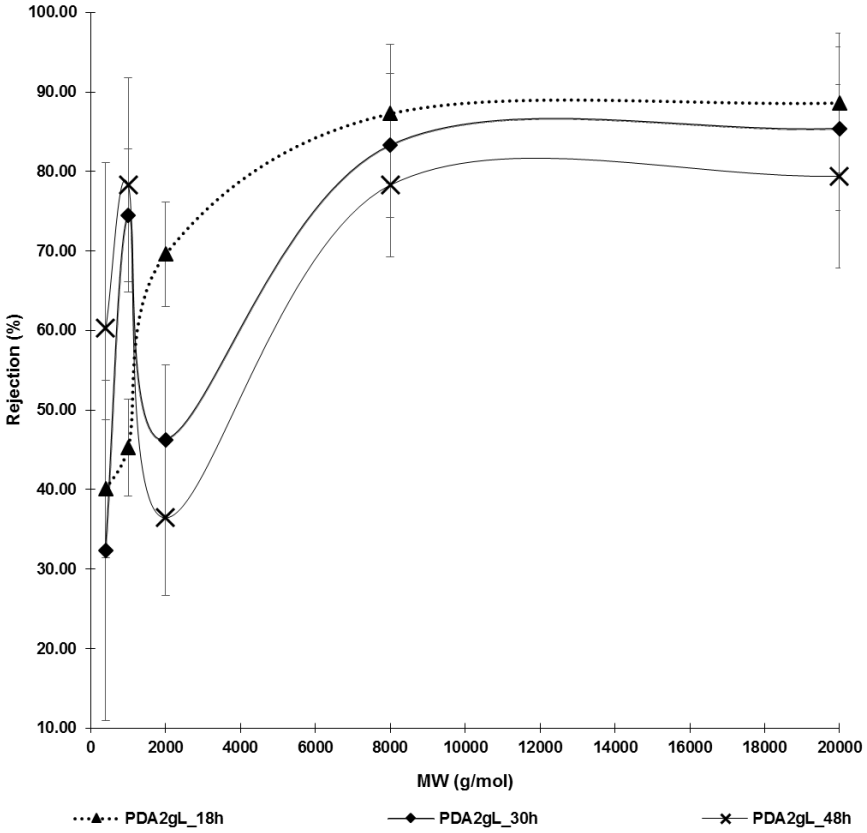

Figure 29. MWCO curve for the single screening of PDA_2gL membranes tested at different coating times.

The morphology of the PDA2gL membranes prepared in the lab is presented in Figure 30. It is perceptible that the more time the membrane was in solution the ticker the membrane fibres get. The small white particles seen, are undissolved polydopamine.

A

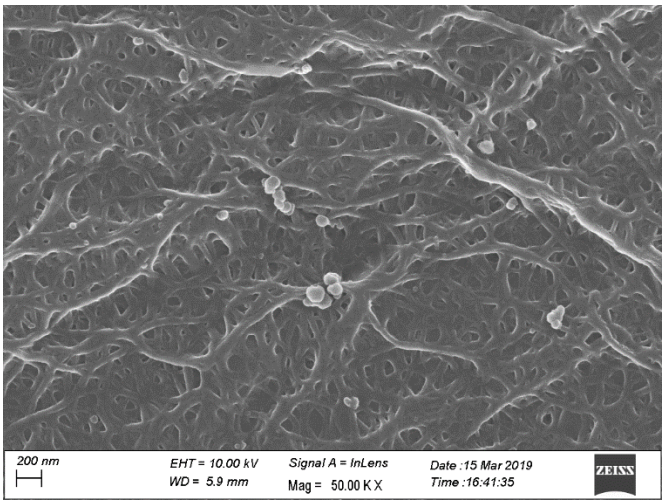

B

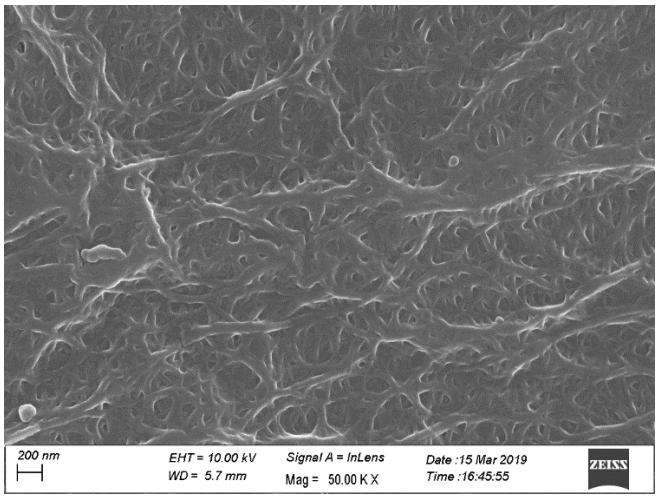

C

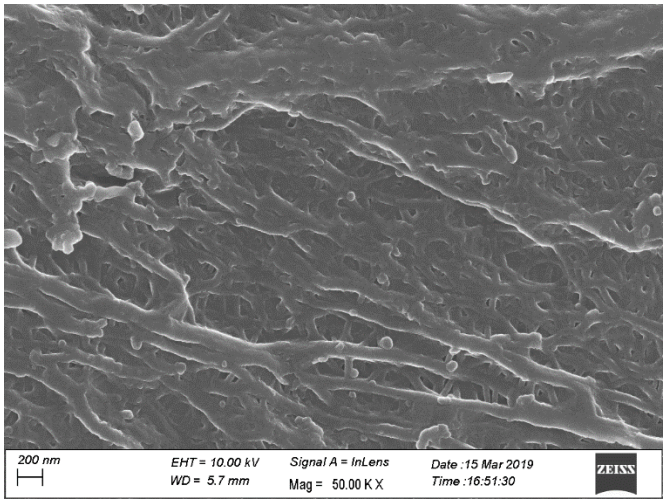

Figure 30. SEM images of membranes. (A) Top-section view of PDA 2gL for 18h at 50000x magnification; (B) Top-section view of PDA 2gL for 30h at 50000x magnification; (C) Top-section view of PDA 2gL for 48h at 50000x magnification.

Concerning PDA4gL, Figure 31, the results are unexpected due to the fact that the PDA48h_4gL membrane was coated for a longer period, therefore, should be tighter and have higher rejection than PDA30h_4gL. One reason can be the fact that because the polydopamine was in higher concentration it couldn't dissolve well in 30h and it blocked some of the pores of the membrane, while the 48h dissolved better in the surface and didn't block the pores. Hence in the 30h coating the retention of bigger PEGs but also of smaller PEGs is higher than the one verified in 48h coating. The rejections are around 60%, 80%, 85% and 90% for PEG1000, PEG2000, PEG8000 and PEG20000, respectively. Therefore the membranes coated with 4gL of polydopamine are not suitable for this studied and were not used in further experiments.

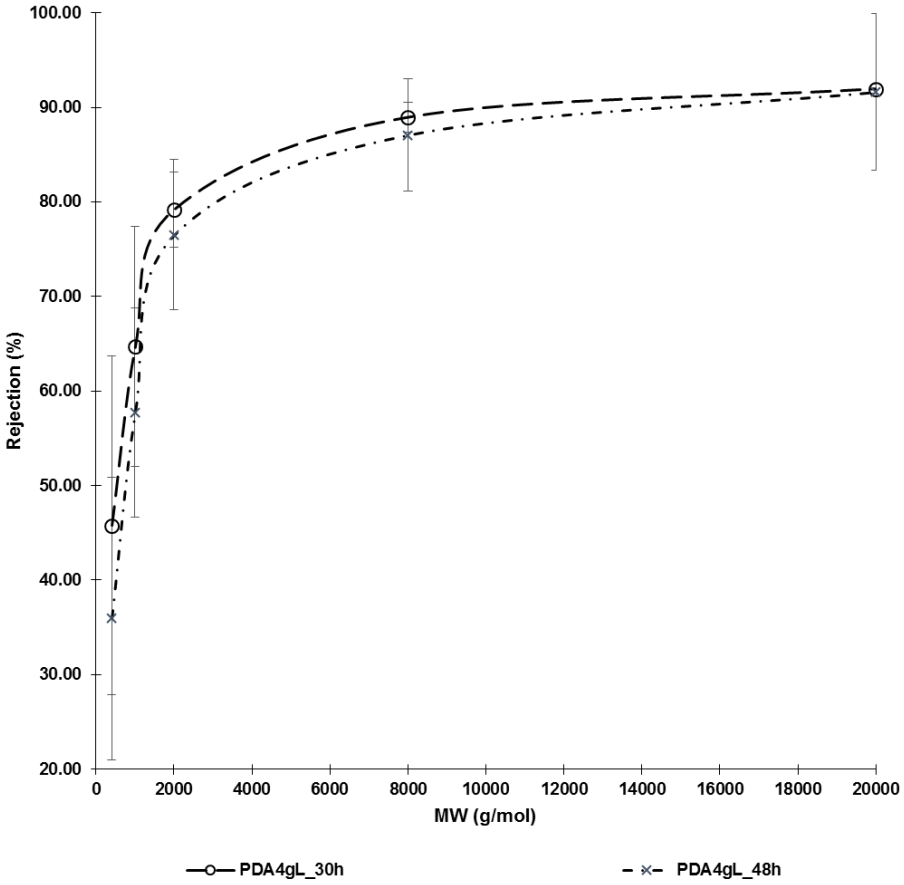

Figure 31. MWCO curve for the single screening of PDA_4gL membranes tested at different coating times.

The SEM images of PDA 4gL 30h and 48h are presented in Figure 32 A and Figure 32 B respectively. As for the PDA 2gL, for the PDA 4gL the more time the membrane was in solution, the better the coating. Hence the PDA4gL coated for 30h has bigger pores than the membrane PDA4gL coated for 48h. But also has it is seen there is much more polydopamine undissolved in the membrane coated for 30h, Figure 32A, than for the membrane coated for 48h, Figure 32B. This can result in interactions between the PDA undissolved and the PEG solution or the PDA blocking the inner pores of the membrane obstructing the passage of PEG and causing an unexpected higher rejection in the PDA 30h than in the PDA 48h.

A

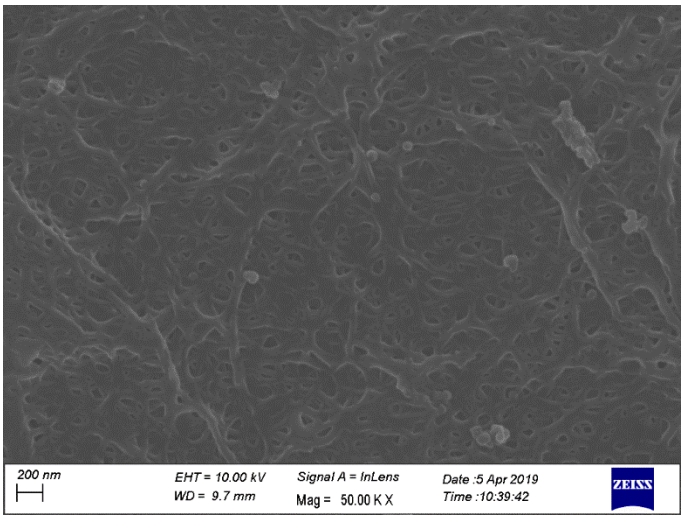

B

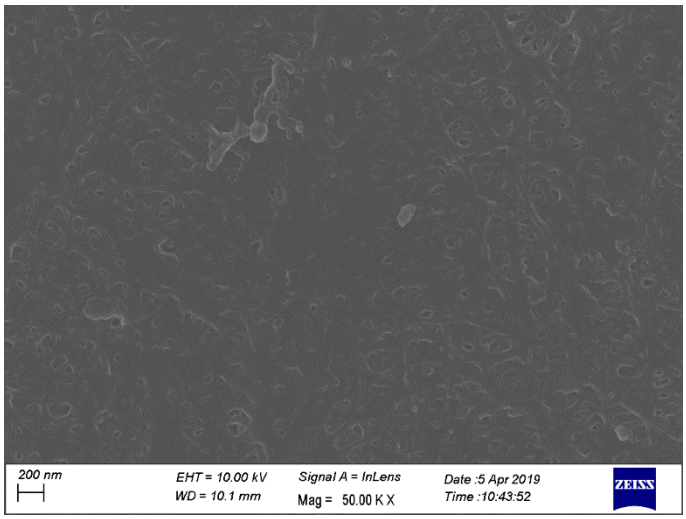

Figure 32. SEM images of membranes. (A) Top- section view of PDA 4gL for 30h at 50000x magnification; (B) Top-section view of PDA 4gL for 48h at 50000x magnification

In general, for most membranes, the rejections reach a steady-state after 3 hours. The results of Table 10 show that in the majority of the membranes, after the stabilization the rejections either maintain or increase due to the membrane compaction, hence at 24h, the membrane is at its highest compaction level. This effect is particularly present in looser membranes (See-Toh., 2008). The most stable membranes are PBIm5j2005 and PEEK. The rejections of PBIj1000 seem to not have stabilized after the usual 3 hours. The membranes coated with PDA also have a higher variation of the rejection when compared with the variation of the PEEK or PBIm5j2005. Nevertheless in most of the cases the rejection after 24h increases which also indicates higher compaction of the membranes (Gibbins, 2002).

Table 10. Rejections after 3h and 24h for the single screening

Membrane code	Rejections (%)					
	R2000(%)		R8000(%)		R20000(%)	
	3h	24h	3h	24h	3h	24h
PBIm5j2005	90.97	90.28	95.15	97.43	98.75	99.26
PBIj1000	73.53	82.29	96.55	99.33	97.60	99.48
PEEK50_5bar	91.50	93.24	98.92	99.33	99.58	99.77
PEEK50_10bar	92.69	91.59	97.75	96.55	99.50	99.58
PEEK50_20bar	94.05	94.02	98.18	98.40	99.46	99.78
PEEK80_5bar	92.84	94.81	99.33	99.44	99.68	99.83
PEEK80_10bar	93.15	80.81	99.48	95.52	99.75	99.03
PEEK80_20bar	95.03	95.94	98.58	98.93	99.60	99.72
PDA2gL_18h_5bar	58.54	66.90	89.80	93.22	95.72	97.41
PDA2gL_18h_10bar	68.36	67.48	86.85	88.85	90.36	94.95
PDA2gL_18h_15bar	69.99	56.84	82.92	88.73	88.08	93.69
PDA2gL_18h	67.55	72.15	83.88	94.95	82.05	97.17
PDA2gL_30h	46.79	52.99	84.28	89.37	86.19	92.88
PDA2gL_48h	45.70	32.25	62.04	84.80	81.17	89.56
PDA4gL_30h	87.31	82.85	94.89	94.25	97.75	98.48
PDA4gL_48h	76.17	82.75	82.47	82.47	93.50	97.64

Figure 33 presents the results of the permeance of all membranes tested in a single screening. Except for PBIm5j2005, PEEK80ºC_5bar and PEEK80ºC_20bar, all the membranes have a decrease in permeance. This decrease is associated with the previously explained pores compaction or with the concentration polarization and membrane fouling that will cause a decrease in the driving force and an increase in resistance near the membrane wall. Hence the greater the permeance decrease, the greater concentration polarization and fouling effect. One way to prevent this initial permeance decline was, before the experiments with the PEG solution start, do a preliminary membrane compaction running pure solvent at a highest transmembrane pressure and then induce a stepwise decrease of the same, instead of running pure solvent only for 2h at a constant transmembrane pressure. (Droli, 2014) Usually, after 5 hours the permeance flux tends to achieve a steady-state mode until the end of the experiment. PDA5bar and PDA2gL_18h present a constant decrease in the permeance and didn't reach the steady-state within 24h. The decrease in permeance was more significant for PEEK_50ºC_5bar, PEEK50ºC_20bar, PDA2gL_48h and PDA4gL_48h, attributed to membrane compaction. In the case of the PBIm5j2005, PEEK80ºC_5bar and PEEK80ºC_20bar the permeance increased in the first 3 hours and then achieved the steady-state. As expected from the rejection results, PEEK membranes have the

highest fluxes due to their looser pores. PEEK50ºC at 5 bar have higher standard deviation since one of the discs is more permeable than the other. On the other hand, PBIm5j2005 is very uniform and the results very consistent with the smallest standard deviations of all experiments. The membranes dried from water at 80 °C have higher permeance than the membranes dried at 50 °C because at 80ºC they are looser. (João da Silva Burgal L. P., 2015) In the case of PDA membrane tested at different pressures, the increasing applied pressure, the driving force of the system, lead to a decrease in the flux. Therefore according to the gel polarization model, the decrease in flux can be attributed to the increase of resistance to the membrane transport and pore shrinkage (N.M. D'Souza, 2003).

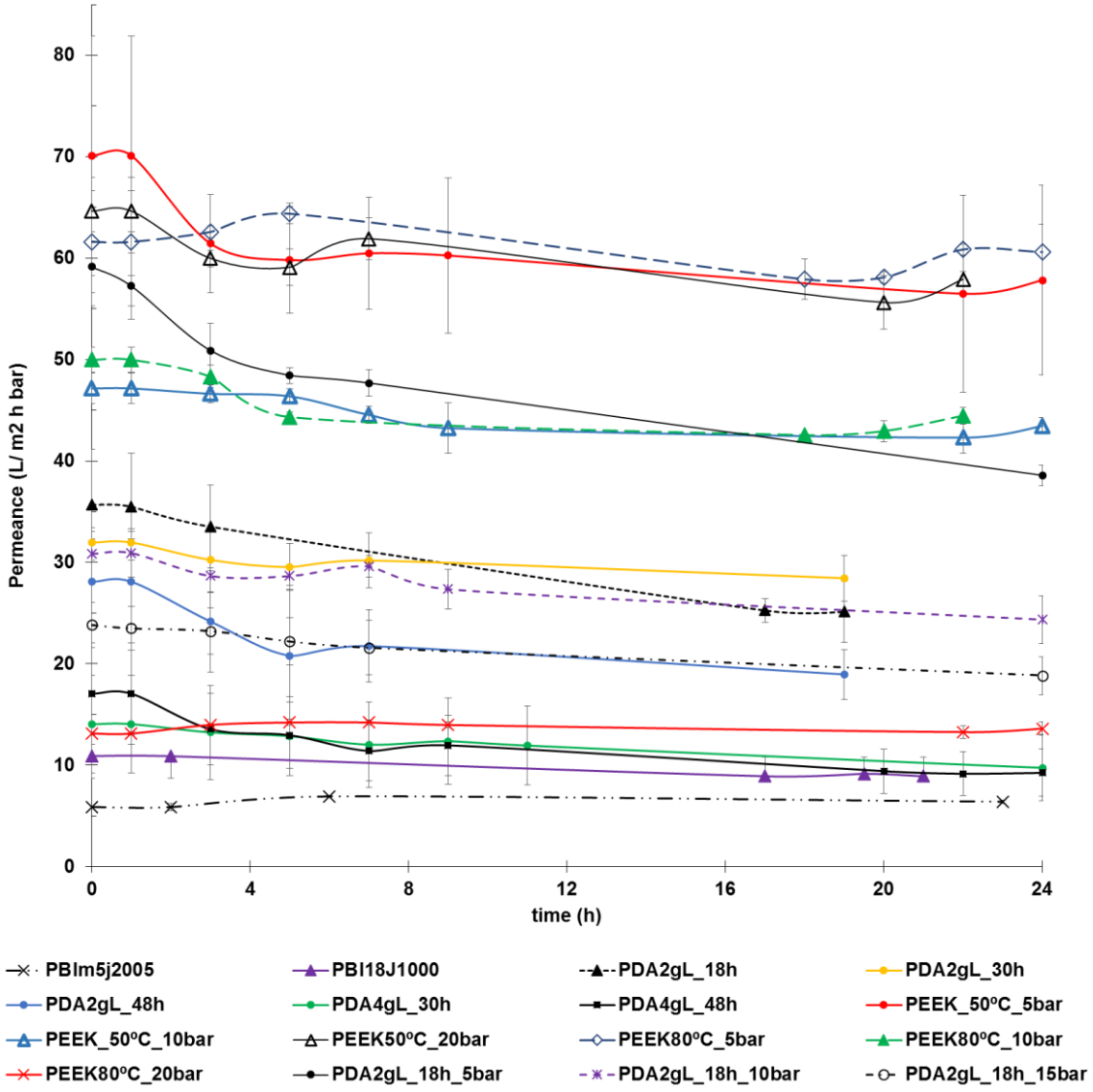

Figure 33. Permeance results of the all the membranes tested in the single screening filtration mode

From the single screening tests, the membranes more adequate to proceed for the cascade membranes are PDA2g/L and PBI, while PDA4g/L and PEEK were not further studied.

4.2. Cascade Screening

In order to improve the separation of the single stage membranes, the cascade configuration was applied. The goal of the cascade diafiltration is to select the best set of membranes able to separate PEG2000 (MW= 2000 $g.mol^{-1}$) from larger PEGs. Hence the OSN membrane needs a rejection close to 100% to intermediate oligomers with 8000Da and larger and the minimum rejection possible for oligomers of 2000Da and lower. The samples were taken and tested in the HPLC for 24 hours. The new configuration (Figure 20, Chapter 3.4.2) has two permeate samples and two retentates which were collected and compared with the standard samples. The set of membranes tested, presented in Table 11, were chosen considering the rejections obtained in the single screening configuration and the model prediction, Chapter 3.4.3. Due to pressure drop from the first stage to the second stage, the second stage needs to have a lower transmembrane pressure than the first stage.

Table 11. Set of membranes tested in cascade mode

Cascade mode		Stage 1	Stage 2
Experiment 1	**Membrane code**	PBIj1000	PDA_2gL_30h
	Transmembrane Pressure (bar)	20	10
Experiment 2	**Membrane code**	PBIj1000	PDA_2gL_30h
	Transmembrane Pressure (bar)	30	10
Experiment 3	**Membrane code**	PDA_2gL_30h	PDA_2gL_30h
	Transmembrane Pressure (bar)	10	5
Experiment 4	**Membrane code**	PDA_2gL_30h	PBIj1000
	Transmembrane Pressure (bar)	20	10

Experiments 3 and 4 were repeated twice, while experiments 1 and 2 due to the low value of flux throughout the experiment were not repeated. In this case the solution is composed of PEG2000, PEG8000 and PEG20000 in the ratio 1.5:1:1 in THF- to simulate the conditions expected after completion of fragment condensation reaction. Figure 34 shows the rejection profile for each membrane tested in the cascade screening for both stages, in which p1 refers to stage 1 and p2 refers to stage 2 (see Figure 20, Chapter 3.4.2)

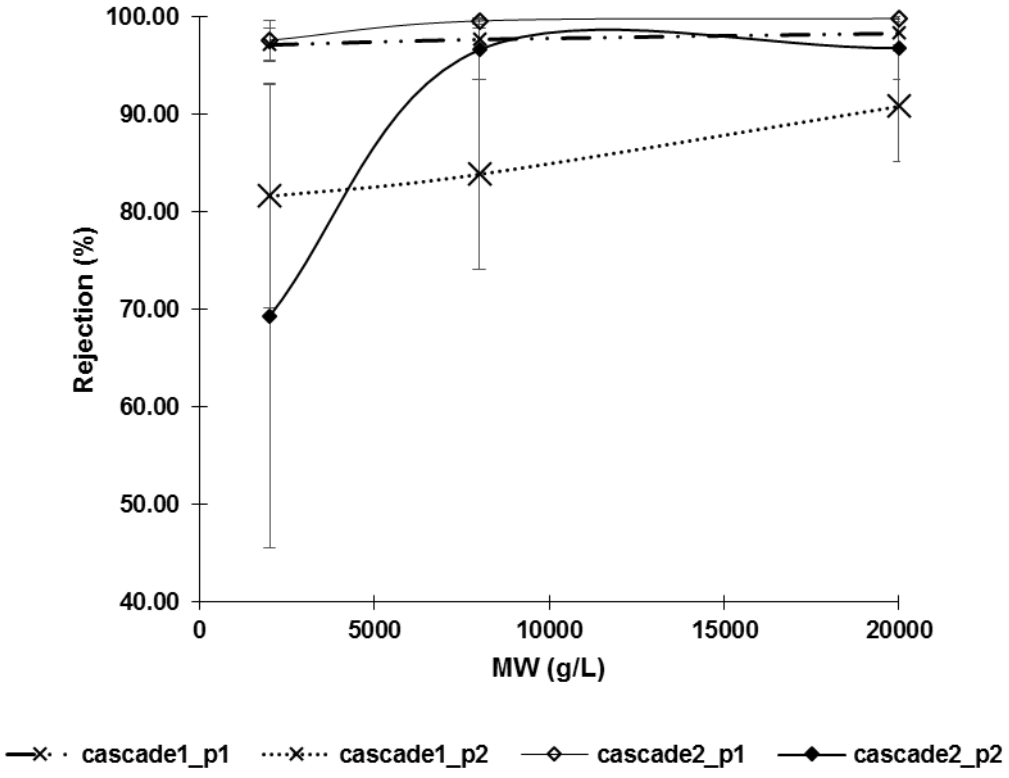

Figure 34. MWCO curve for the cascade screening tests experiments 1 and 2.

The first experiment, Figure 34, cascade both stages present a similar rejection to the solution. The first stage has a rejection of about 97-98% for all PEGs while the second stage has a rejection of 82%, 84% and 91% for PEG2000, PEG8000 and PEG20000, respectively. Therefore neither stage was able to have a good separation of PEG2000 from PEG8000 and PEG20000. The permeance, Figure 35, in this experiment was also too low for stage1 and was kept constant, due to the fact that PBI membranes are very stable. While the stage 2 with PDA membrane suffered a decrease in permeance from 32 $L/m^2.bar^{-1}.h^{-1}$ to 10 $L/m^2.bar^{-1}.h^{-1}$ due to membrane compaction. In order to increase the flux and to improve the separation of PEG2000 from PEG8000 and PEG20000, it was necessary to increase the pressure of the first-stage. After the pressure modification, as expected and from Figure 35, the increase in pressure lead to an increase in flux.

Although the flux increased in the second cascade experiment, the membrane of the first stage in too tight and rejects every MW PEG, Figure 34. However, the second stage has a better separation than the previous experiment, with a rejection of 69% for PEG2000 and around 98% for PEG8000 and PEG20000. This improvement of the membrane in the second stage is more notorious in the first two hours, with a rejection of 40% for PEG2000 and above 95% for the remaining PEGs. But after the 3rd hour, the

membrane suffers sudden compaction, becomes too tight and starts rejecting 90% PEG2000. In this experiment, the flux decreased constantly with the permeance of the first stage lower than the second stage.

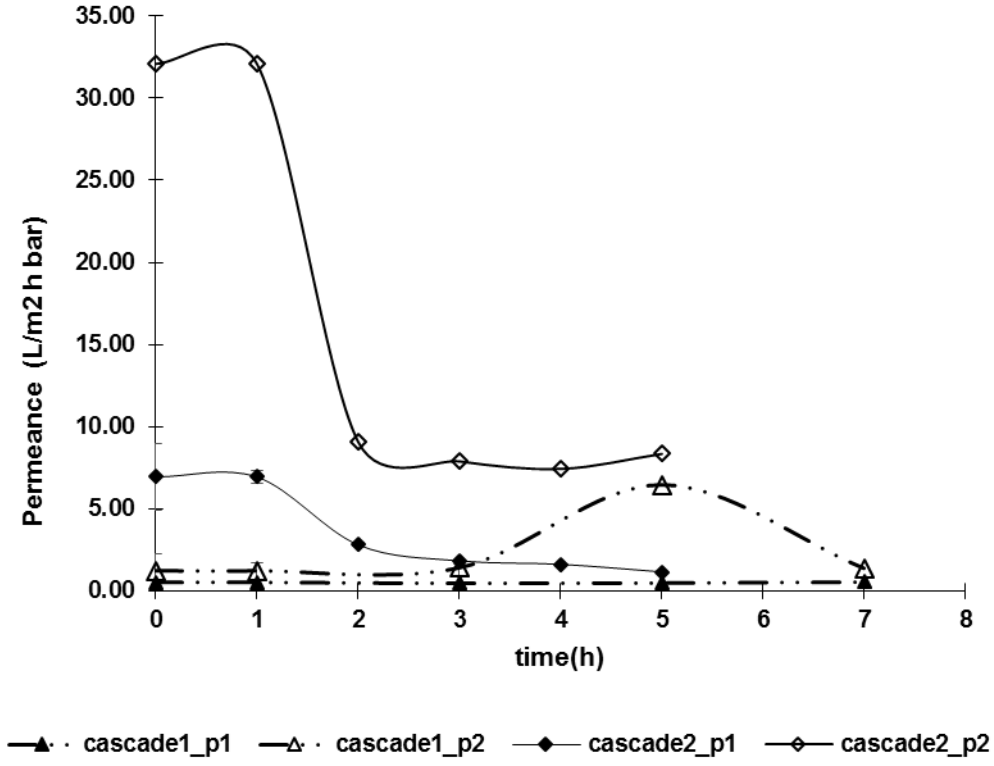

Figure 35. Permeance of the first two experiment cascade screening tests.

The third cascade experiment was repeated twice and the results are not consistent regarding the second stage. The first stage membrane is too tight and rejects 89% of PEG2000 and has a rejection above 95% for PEG8000 and PEG20000. The second stage membrane had an average rejection of 64% for PEG2000, 74% and 79% for PEG8000 and PEG20000, respectively, Figure 36.

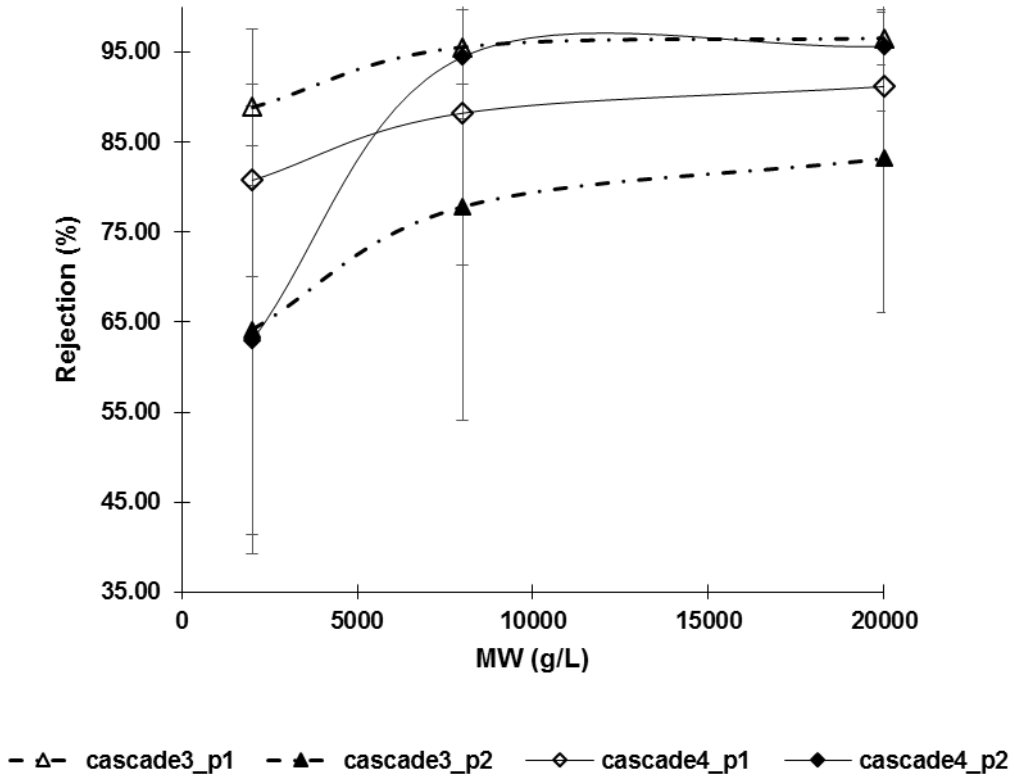

Figure 36. MWCO curve for the cascade screening tests experiments 3 and 4.

The inaccurate results and high errors for the second stage are due to the fact that in the first trial, the second membrane rejected 80% PEG2000 and 90% above for the remaining PEGs, while for the second trial the rejection of the second stage for PEG2000, PEG8000 and PEG20000 was of 50%, 66% and 74%, respectively. This inconsistency may be an indication of the non-uniformity of the polydopamine membrane coating. Another difference in the experiments for the second stage is the fact that for the first trial, the rejection started in 37% for PEG2000, 63% for PEG8000 and 80% for PEG20000. In the third hour, quick compaction of the membrane leads to an increase of rejection, 72% for PEG2000, 89% for PEG8000 and 93% for PEG20000 that increased to 98% for all PEGs after 14h. The permeance of the second stage, Figure 37, is higher than the one of the first stage, still, after the third hour, it suffers a decrease for both stages in the first trial. In the second trial, the first stage rejected everything while the second stage rejected 50%, 66% and 74% for PEG2000, PEG8000 and PEG20000. Although the pressure was the same in both experiments, the second trial has average permeance 33% lower than the ones obtained for the second stage due to the non-uniformity of the PDA membranes.

The last cascade experiment was also repeated twice and the results are not consistent with the second trial results being closer to the expected. In this trial, the first membrane rejected 78% for PEG2000 and about 90% for the remaining PEGs, while the second stage has a rejection of 50% for PEG2000 and above 90% for PEG8000 and PEG20000. The first stage has an initial decrease from 0.12 L/h to 0.08 L/h but then it rises again to the initial value. The second stage has an increase from 0.07 L/h to 0.09 L/h, but afterwards, it has a sudden decrease to 0.03L/h. The permeance has the same behaviour has the flux in both stages.

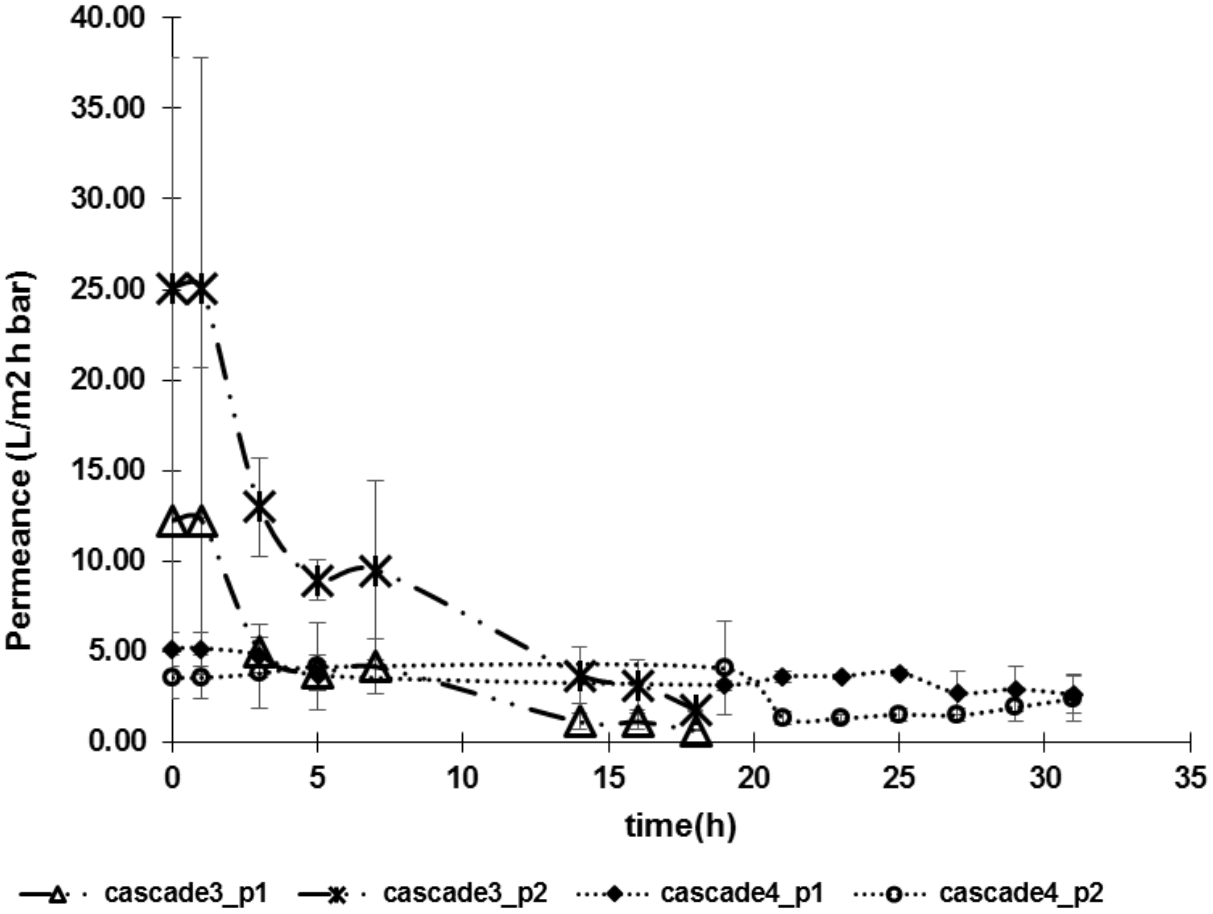

Figure 37. Permeance of the last two experimenrts of cascade screening tests, each exeriment was repeated twice

Afterwards, the cascade results show that the best combination of membranes for rejection is experiment 4 with PDA at 20 bar in the first stage and PBIj1000 at 10 bar for the second stage.

4.3. Diafiltration Screening

This chapter presents the results of both configurations of diafiltration, (see Figure 21 and Figure 22 in Chapter 3.4.3). For both cases PEG8000 represents the simulation of the first coupling, in which the total peptide structure would have around 8000Da while the PEG20000 corresponds to the second fragment coupling in which the peptide structure would have 20000Da while the fragments always have around 1.5-2k Da.

4.3.1. First configuration

In the first diafiltration configuration, although the volume of each cell was about 15.5mL, the volume of each stage was 30 mL while the volume of the feed solution was 60mL. Therefore the total volume of the system, which corresponds to 1 vol, is 120 mL with the first stage 90mL and the second stage 30mL. Just as in the cascade, the PEG solution had a concentration of concentration (g/L) of 1.5:1:1 for PEG2000:PEG8000:PEG20000. Figure 38 and Figure 39 show the results for the purity and yield obtained in the diafiltration process for PEG8000 and PEG20000 using the configuration of Figure 21 (Chapter 3.4.3). This configuration required the addiction of 0.720L of pure THF. As it can be seen for PEG8000, Figure 38, the model predicted a starting purity of 40% while the experimental purity is 60%. One of the causes can be the accuracy of measuring, in both cases overweighting. After 6 vols all the feed solution had been washed out and the purity reached 90% as predicted by the model. On the other hand, the final yield is only 10%, while the prediction was of 40%. This low yield may be due to mass transfer problems.

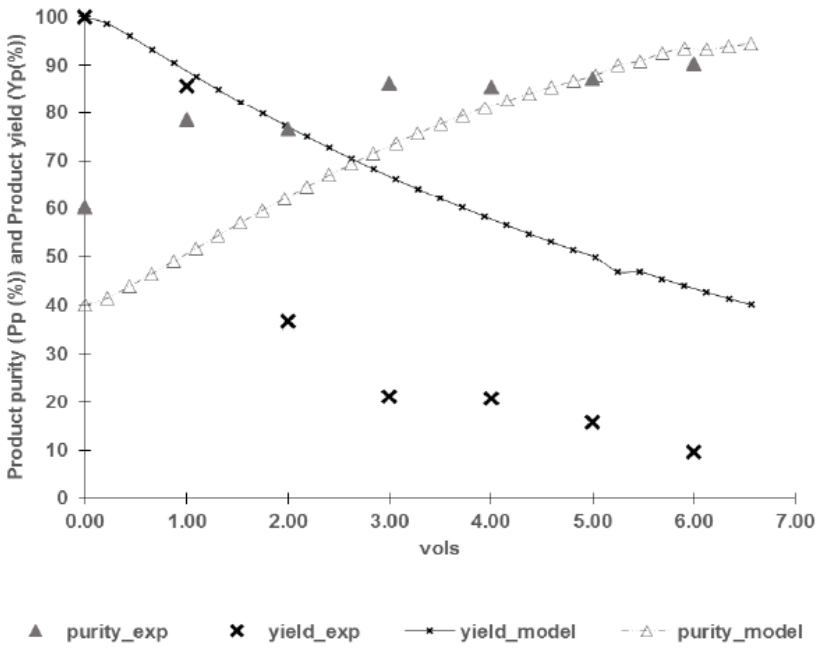

Figure 38. Calculated and experimental purity and yield for PEG8000.

For the PEG20000, Figure 39, the purity predictions fit in the experimental results. The yield should have reached 70% after 6 vols according to the model, but the experiments show a huge drop and after 6 vols is less than 10%.

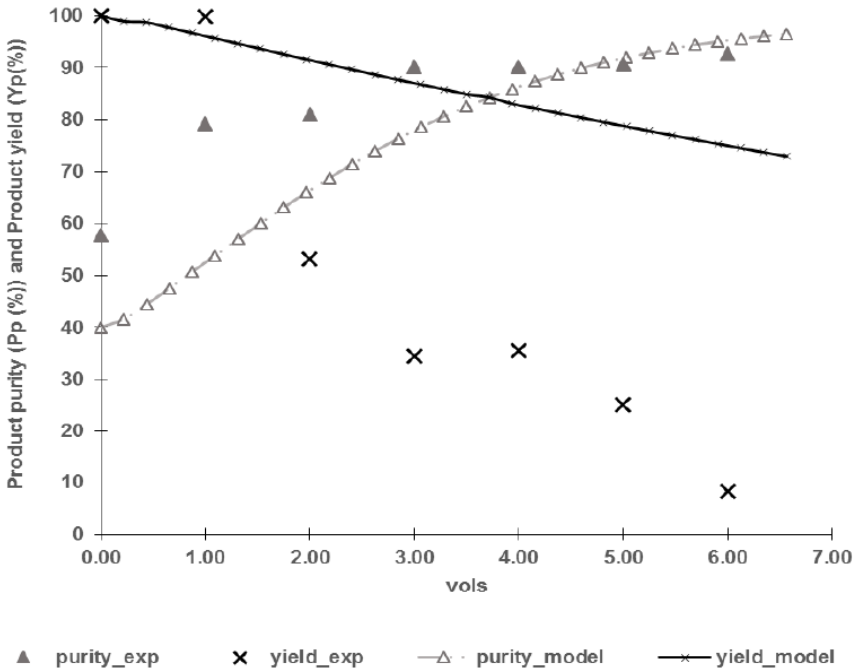

Figure 39. Calculated and experimental purity and yield for PEG20000.

During this experiment it was verified precipitation of PEG inside the membrane cell, Figure 40, that may have led to low mass transference hence low yield.

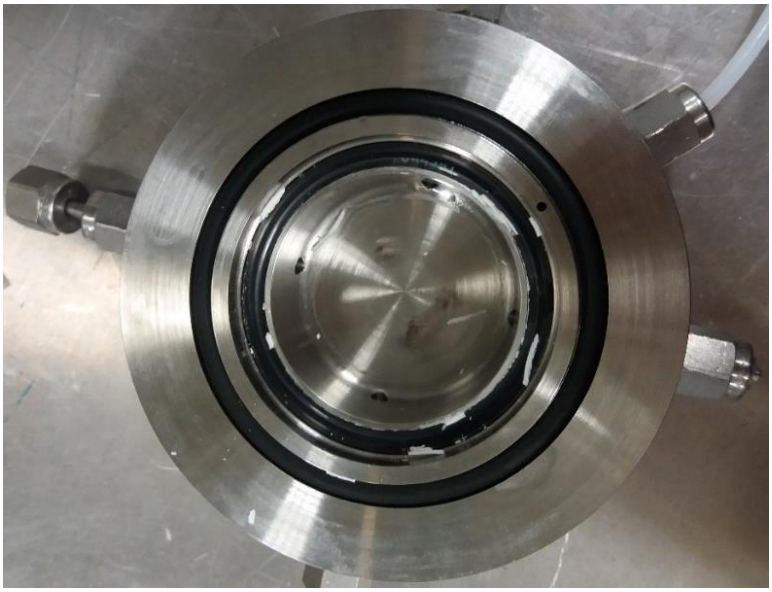

Figure 40. PEG precipitation

4.3.2. Second configuration

The new configuration, Figure 22 Chapter 3.4.3, has two pumps to promote mixing and circulation of the liquid in order to increase the mass transference and therefore the yield obtained. PEG precipitation was not verified. In this case, the volume of each stage was 60 mL while the volume of the feed solution was 75mL. Therefore the total volume of the system, which corresponds to 1 vol, is 195 mL with the first stage 135mL and the second stage 60mL. As previously, the PEG solution had a concentration of concentration (g/L) of 1.5:1:1 for PEG2000:PEG8000:PEG20000. Figure 41 and Figure 42 show the results for the purity and yield obtained in the diafiltration process for PEG8000 and PEG20000 using the configuration of Figure 21, Chapter 3.4.3. For this configuration, 6 vols required the addiction of 1.170L of pure THF, half litter more than the previous diafiltration. This time the initial experimental purity matches the model prediction for both PEG8000 and PEG20000. Unexpectedly after 6 vols the experimental yield reached 30% while the model predicted 95%. Due to this discrepancy and the amount of solvent required the experiment was stopped. Even though the experimental yield is 60% lower than the model prediction, the purity was only 10% underestimated by the model. Hence after 6 vols, the experimental purity is 60% while the model predicted 50%.

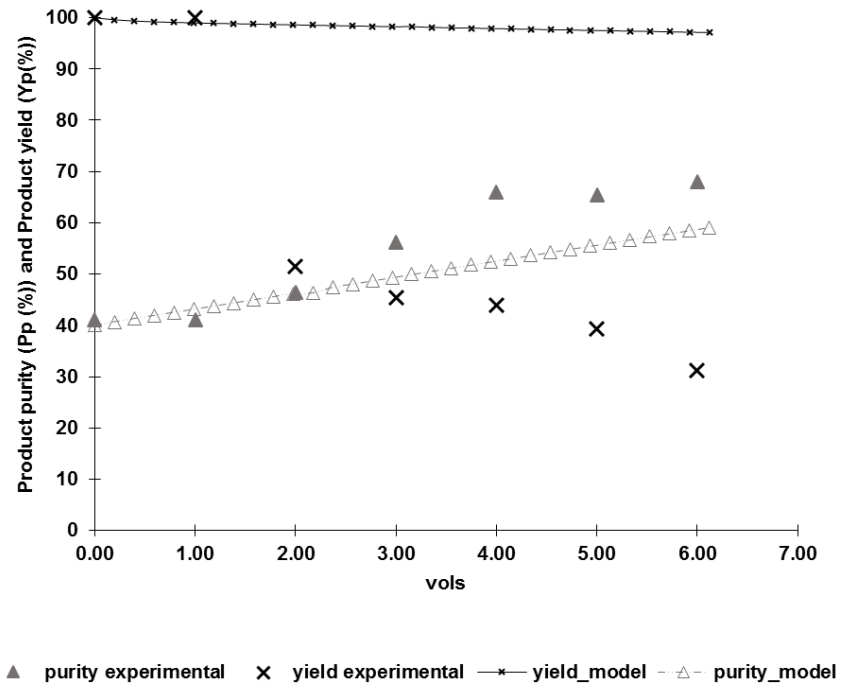

Figure 41. Calculated and experimental purity and yield for PEG8000.

Similar behaviour is verified for the PEG20000 with the model prediction of 60% and 95% for purity and yield respectively after 6 vols, while the experiments show the purity is 70% and the yield is 40%.

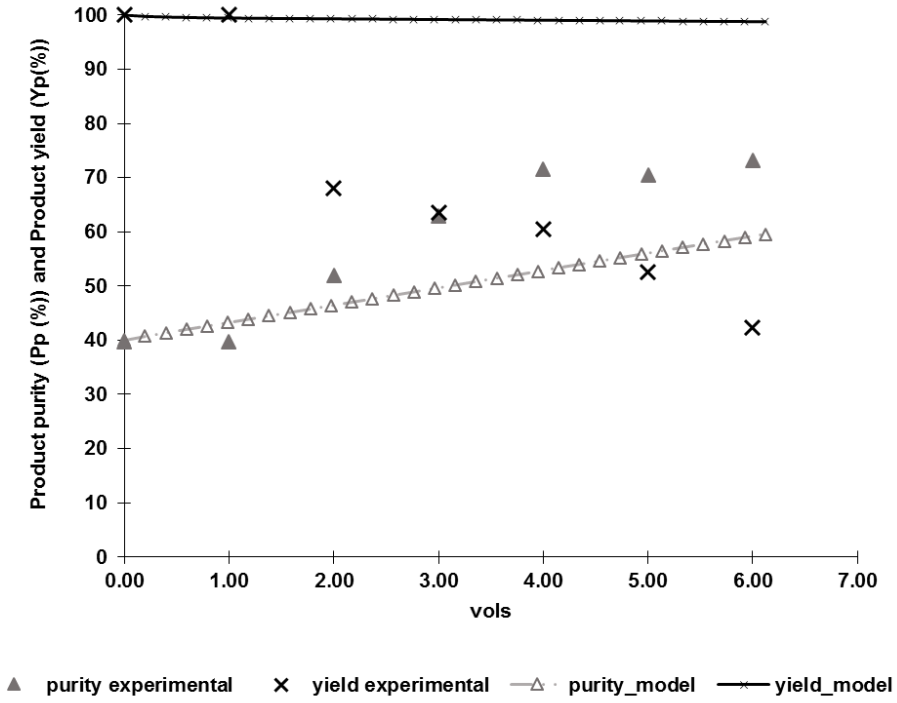

Figure 42. Calculated and experimental purity and yield for PEG20000

To understand the mass transfer in both configurations, it was necessary to calculate the Reynolds number. The diameter of the impeller is 3 cm and the agitation speed was 500rpm (rotations per minute). The Reynolds number is the first configuration depends on the diameter and speed velocity of the stirrer and on the density and viscosity of the solution. It was used the data of THF instead of the solution. In the second configuration, the Reynolds number on the entry port of the cell depends on the diameter of the tube which was ¼ inch, on the speed of permeate which depends on the area of the tube and the flow of the pump. The pump operated at 20% of its total power, therefore considering Figure 43 present in Annexe 0, the flow rate, Q, is approximately 90 L/h. The viscosity and density were assumed to be the viscosity and density of THF. (DDBST GmbH, 2019) The results of the dimensionless numbers for the analysis of mass transference are presented in Table 12.

Table 12. Dimensionless Numbers

Configuration	**Dimensionless number**		**Region**
1st diafiltration	Re	8813.66	Turbulent
	Np	4.00	----------
	P (W)	0.01	----------
2nd diafiltration	Re	9817.93	Turbulent

According to the calculations both configurations have turbulent flow, still the fact that the values for viscosity and density were approximate the results are not accurate. Reynolds for the first configuration is 8k while the second diafiltration has a Reynolds of about 10k which means that the flow is turbulent. As expected the first configuration has more mass transfer problems than the 2nd configuration proved by its lower Reynolds number indicating the viscosity of the fluid has larger impact than the density of the fluid. Considering that the stirrer can be approximate to a Straight-blade turbine, according to Figure 3 Chapter 2.1.2 considering curve 2, the power number is 4, which corresponds to an impeller power of 0.011 Watts.

5 . Conclusions and future work

This work proposed the integration of a membrane cascade as well as diafiltration process to improve the separation performance realized by a single membrane in the purification of peptides. As a case study it was used a solution of containing oligomers of different MW that match the MW of the peptides, sizing 8000Da and 20000Da, by-products and impurities, of size 2000Da. This approximation simulates the MW of the fragments and by-products of reaction, but it doesn't take in consideration the fact that amino acids tend to have a lot of interactions with the medium they are being prepared in. Hence the results are not accurate for a real life application and the aminoacids and fragments would interact with the membrane and most likely decrease the rejection.

The single screening configuration tested different membranes in different pressure conditions membranes, including PBI, PEEK and membranes coated with 2g/L and 4g/L polydopamine. The results showed that neither of the PEEK membranes, neither the coating with 4g/L of polydopamine could separate the PEG2000 from larger PEGs, hence these membranes were not further studied.

Using the MATLAB simulations and the results of single screening it was possible to predict that from the remaining membranes, the best combinations would be using PBI and 2g/L of polydopamine. The experimental results showed that PDA2g/L_30h at 20 bar in the first stage and PBIj1000 at 10 bar for the second stage have the best separation, with the second stage rejecting about 95% PEG8000 and PEG20000, and 68% PEG2000. These membranes were applied in the diafiltration mode in the same above conditions.

For the first diafiltration configuration, the MATLAB simulations predicted yields between 40-70% and purities above 90% after 6 vols, but the experimental results don't fit in the predictions with yields below 10% after 6 vols. The second diafiltration configuration improved the experimental yield results to 30-40% because the mass transference was improved by placing pumps in each cell instead of a magnetic stirrer, but still, the model predicted yields above 90%. The experimental purity was around 60-70%, which is 10% overestimation according to the model.

According to the literature, the diafiltration is a process that increases the purification of the APIs, but it was concluded that the diafiltration performance also depends on the membranes selected. On the contrary to the membranes studied, for the purification be efficient, the membranes should have had a rejection close to 100% for PEG8000 and PEG20k, but they should have the minimum rejection possible, preferably close to 0% for PEG2000 and lower, in order to have complete separation. Hence to better purify the necessary APIs, different membranes must be developed and studied.

6 . References

A.Piry, A. W. (2012). Effect of membrane length, membrane resistance, and filtration conditions on the fractionation of milk proteins by microfiltration. *Journal of Dairy Science, Volume 95*(Issue 4), pp 1590-1602. Retrieved from https://www.sciencedirect.com/science/article/pii/S0022030212001245

Ali K. Alshehri, Z. L. (2015). Attainability and minimum energy of multiple-stage cascade membrane systems. *Journal of Membrane Science, 495*, pp. 284–293.

Bachem AG. (2016). *Coupling Reagents.* Global Marketing, Bachem Group. Retrieved from http://documents.bachem.com/coupling_reagents.pdf

Baker, R. W. (2004). *Membrane Technology and Applications* (2nd edition ed.). John Wiley and Sons, Ltd.

Benedict, M. P. (1981). *Nuclear Chemical Engineering* (2nd Edition ed.). McGraw-Hill.

Burgal, J. P. (2016). *Development of Poly (ether ether ketone) Nanofiltration Membranes for Organic Solvent Nanofiltration in Continuous Flow Systems.* Dissertation, Imperial College London, Department of Chemical Engineering.

Byrnes, M. W. (1994). Methods in Molecular Biology. Em M. W. Byrnes, *Methods in Molecular Biology* (Vol. 35, pp. Ch I, Ch II, Ch V and Ch XI). Totowa NJ: Humana Press Inc.

Chudacek, M. W. (1985). Impeller power numbers and impeller flow numbers in profiled bottom tanks. *Industrial & Engineering Chemistry Process Design and Development, 24*, pp. 858-867.

Daniel Carbajo, P. F.-F. (2019). Pseudo-Wang Handle for the Preparation of Fully Protected Peptides. Synthesis of Liraglutide by Fragment Condensation. *Organic Letters, 21*, pp. 2459−2463.

DDBST GmbH. (2019, 08 08). *Dortmund Data Bank*. Retrieved from Dynamic Viscosity of Tetrahydrofuran: http://www.ddbst.com/en/EED/PCP/VIS_C159.php

Dolan, C. S. (2003). *Success with Evaporative Light-Scattering Detection.* LC Troubleshooting.

Droli, L. G. (2014). *Encyclopedia of Membranes: Membrane Compaction.* Springer-Verlag Berlin Heidelberg. doi:DOI 10.1007/978-3-642-40872-4_1404-2

Fane, A. (2005). Ch4 Module design and operation. In A. F. Schafer, *Nanofiltration Principles and Applications* (1st Edition ed., pp. pp. 67-88). Oxford Elsevier Ltd.

Gibbins, E. D. (2002). Observations on solvent flux and solute rejection across solvent resistant nanofiltration membranes. *Desalination, 147*, pp.1-3.

Irina Boyanova Valtcheva, A. G. (2015). *Polybenzimidazole Membranes for Organic Solvent Nanofiltration - Formation Parameters and Applications.* Imperial College London , Department of Chemical Engineering, London.

J.H. Jiang, L. Z. (2011). Surface Characteristics of a Self- Polymerized Dopamine Coating Deposited on Hydrophobic Polymer Films. *Langmuir, 27*, pp. 14180–14187.

João da Silva Burgal, L. P. (2015). Organic solvent resistant poly (ether-ether-ketone) nanofiltration membranes. *Journal of Membrane Science, 493*, pp. 105.116.

João da Silva Burgal, L. P. (2016). *Towards greener membrane production: using low-toxicity solvents for the preparation of PEEK nanofiltration membranes.* Dissertation, Imperial College London, Department of Chemical Engineering, London.

Junfeng Pan, J. L. (2016). *U.S.A Patent No. US 9 260 474 B2, Method for solid phase synthesis of liraglutide.*

Kent, S. B. (1988). Chemical Synthesis of Peptides and Proteins. *Annual Reviews Biochemistry, 57*, pp. 957-989.

Kovács, Z. (s.d.). *Diafiltration.* Institue of Bioengineering and Process Engineering, Department of Food Engineering. Budapest, Hungary: Szent Istvan University.

Kyoung-Yeol Kim, E. Y.-Y.-J.-M. (2014). Polydopamine coating effects on ultrafiltration membrane to enhance power density and mitigate biofouling of ultrafiltration microbial fuel cells (UF-MFCs). *Water Research, 54*, pp. 62-68.

Lin, J. &. (2007). Nanofiltration membrane cascade for continuous solvent exchange. *Chemical Engineering Science, 62 (10)*, pp. 2728-2736.

Livingston, A. N. (2009, April). Molecular separation: the new frontier in liquid fitration. *The Chemical Engineer*, pp. 34-36.

McCloskey, B. P. (2010). Influence of polydopamine deposition conditions on pure water flux and foulant adhesion resistance of reverse osmosis, ultrafiltration, and microfiltration membranes. *Polymer, 51*, pp. 3472-3485.

Mulder, M. (1996). Ch I Introduction. In *Basic Principles of Membrane Technology* (pp. pp. 1-21). Netherlands, Dordrecht: Kluwer Academic Publisher.

Mulder, M. (1996). ChII Materials and materials properties. In *Basic Principles of Membrane Technology* (2nd Edition ed., pp. pp. 22-10). Dordrecht: Kluwer Academic Publisher.

Mulder, M. (1996). ChVIII Module and Process design. In *Masic Principles of Membrane Technology* (2nd Edition ed., pp. pp. 465-523). Netherlands, Dordrecht: Kluwer Academic Publisher.

N.M. D'Souza, D. W. (2003). Whey ultrafiltration: Effect of operating parameters on flux and rejection. *5th International Membrane Science and Technology Conference*.

Nanofiltration Separations Part 2 (Nanotechnology). (2019, 02 25). Retrieved from http://what-when-how.com/nanoscience-and-nanotechnology/nanofiltration-separations-part-2-nanotechnology/

Novabiochem. (2014). *Fmoc resin cleavage protocols.* EMD Millipore.

Patrizia Marchetti, M. F. (2014). Molecular Separation with Organic Solvent Nanofiltration: A Critical Review. *Chemical Reviews, 14*, pp. 10735−10806.

Piers Gaffney, A. L. (2017). *Patent No. WO 2017/042583 Al, Defined monomer sequence polymers.*

R.W., B. (2004). Ch 1 Overview of Membrane Science and Technology. *Membrane Technology and Applications*, 10.

Science Direct. (2019, 08 20). *Diafiltration*. Retrieved from Learn more about Diafiltration: https://www.sciencedirect.com/topics/biochemistry-genetics-and-molecular-biology/diafiltration

ScienceDirect. (2019, 08 20). *Diafiltration*. Retrieved from Learn more about Diafiltration: https://sciencedirect.com/topics/engineering/diafiltration

See-Toh., S. M. (2008). Controlling molecular Weight Cut-Off for highly solvent stable organic solvent nanofiltration (OSN). *Journal of Membrane Science, 324*, pp. 220-232.

Silva, A. (2012). *A simple closed-loop membrane process for the purification of active pharmaceutical ingredients.* Master Thesis, Imperial College of London, Department of Chemical Engineering and Chemical Technology.

Sinnott, R. K. (2005). Coulson & Richardson's Chemical Engineering. Em R. K. SINNOTT, *Chemical Engineering Design* (Vol. 6, pp. pp. 470- 476, 664). Elsevier.

Spear, M. (2006). *Separations in Flux*. Retrieved 03 20, 2019, from https://www.chemicalprocessing.com/articles/2006/025/

Tarfah I.Al-Warhi, H. M.-H.-F. (2012, 04). Recent development in peptide coupling reagents. *Journal of Saudi Chemical Society, 16*(2), pp. 97-116.

Termofischer Scientific. (2019, 03 18). *Peptide Synthesis*. Retrieved 03 18, 2019, from Termofischer Scientific Home: https://www.thermofisher.com/uk/en/home/life-science/protein-biology/protein-biology-learning-center/protein-biology-resource-library/pierce-protein-methods/peptide-synthesis.html

Thermofisher Scientific. (1998). *Technical Bulletin: Cleavage, Deprotection, and Isolation of Peptides after Fmoc.* Retrieved from http://tools.thermofisher.com/content/sfs/brochures/cms_040654.pdf

Tomé, R. d. (2016). *Development of Polydopamine Coated Membranes: Fabrication, Characterization and Morphology.* Instituto Superior Técnico de Lisboa. Técnico de Lisboa.

UK Gov. (2019, 04 19). *the global diabetes community*. Retrieved from the global diabetes community: https://www.diabetes.co.uk/body/glucagon.html

V. Ball, D. F. (2012). Kinetics of polydopamine film deposition as a function of pH and dopamine concentration: Insights in the polydopamine deposition mechanism. *Journal of Colloid and Interface Science, 186*(1), pp. 366-372.

Vandezande, P. G. (2008). Solvent resistant nanofiltration: separating on a molecular level. *Chemical Society Reviews, 37 (2)*, pp. 365-405.

Villani, S. &. (1979). *Uranium enrichment.* New-York: Springer-Verlag.

Visp, L. L. (2017). *China Patent No. EP 3 196 206 A1, Method for preparation of liraglutide.*

Waters . (2019). *The Science of What's Possible*. Retrieved from How Does High Performance Liquid Chromatography Work?: https://www.waters.com/waters/en_GB/How-Does-High-Performance-Liquid-Chromatography-Work%3F/nav.htm?cid=10049055&locale=en_GB

Wen Hou, X. Z.-F. (2017). Progress in Chemical Synthesis of Peptides and Proteins. *Trans. Tianjin Univ. Review, 23*, pp. 401-419.

Wildemuth, R. M. (2004). Membrane separation in solvent lube dewaxing. *Enviromental Progress & Sustainable Energy, 20*(1), pp.12-16.

Zambujo Pé-Leve, I. (2012). *Evaluation of High Pressure Effects on Ultrafiltration Process Applied to Aqueous Inkjet Colorant.* Lisboa Portugal: IST.

陈友金, 潘. 覃. (2014). *China Patent No. CN 104045705 A, Synthetic method of liraglutide.*

7. Annexes

7.1 Matlab Code used for the Cascade and diafiltration simulations

```
function memb

    tspan=0:10:300
    x=[];
    y=[];
    vols=[];
    conc=[];
    mass=[];
    mass2=[];
    pt=[];
    purity=[];
    yield=[];
    purity2=[];
    yield2=[];
    single=[];
    single_i=[];
    single_j=[];
    mm=[];
    conc1=[];
    conc2=[];
    conc3=[];
    conc4=[];
    nc1=[];
    nc3=[];
    nm1=[];
    nm3=[];
    mv1=[];

        x0=[1.5 0 1 0]; % c1ismall fragments=1.5mol and c1_Hub=1 mol
        options = odeset('RelTol',1e-5,'AbsTol',1e-7);
        %AbsTol is x4-x5 in modulus
        %RelTol is (x5-x4)/x4 in modulus

     [t,x] = ode45(@odetest,tspan,x0,options)

        for i=1:length(tspan)
            Vf=0.400; %feed tank =0.2L,stage1=0.1L and stage2=0.1L
            A=0.0014;%m2
            J= 8;%L/(m2 h bar)
            p= 20;%bar
            F1= J*A*p; %L/h
            rc=0.5; %rc=F3/F1
            F3= rc*F1;
            F2= F1-F3;
            v= (tspan(i)*F2)/Vf;
            vols= [vols,v];

             %j=PEG2000, i=PEG400
             %A(:,n) is the nth column of matrix A.
             %A(m,:) is the mth row of matrix
        end

      for a=1:length(vols)
```

```
                    c1=x(:,1);
                    conc1=[conc1, c1];
                    c2=x(:,2);
                    conc2=[conc2,c2];
                    c3=x(:,3);
                    conc3=[conc3, c3];
                    c4=x(:,4);
                    conc4=[conc4,c4];

                    %normalized concentration
                    n1=x(:,1)/x(1,1);
                    nc1=[nc1, n1];
                    n3=x(:,3)/x(1,3);
                    nc3=[nc3,n3];

                    %but if we recover the 2nd stage
                    V1=0.2+0.1;%L feed tank has 100 mL and each
membrance cell+ tubing is 100 mL
                    V2=0.1;%L
                    mm=[ x(:,1)*V1,x(:,2)*V2,x(:,3)*V1,x(:,4)*V2];
%mass in grams
                    mm2=mm(:,3)+ mm(:,4); %m_PEG2000 final
                    mm1= mm2+ mm(:,2)+ mm(:,1);% m_PEG2000 final+
m_PEG400 final

                    p2= (mm2./ mm1)*100;
                    purity2=[purity2,p2]; %of PEG2000

                    y2=(mm2./mm(1,3))*100;
                    yield2=[yield2,y2]; %of PEG2000

                    %normalized mass
                    n_m1=mm(:,1)/mm(1,1);
                    nm1=[nm1, n_m1];
                    n_m3=mm(:,3)/mm(1,3);
                    nm3=[nm3,n_m3];
            end

    figure
    subplot(1,2,1)
    plot(vols,c1,'g-*',vols,c3,'y-o')
    xlabel('vols');
    ylabel('Concentration 1st stage (g/L)');
    title('1stage profile');
    %axis([0 13 0 1])
    legend('Cr1-2000','Cr1-8000')
    %set(gca, 'XLim', [0, 14], 'XTick', 0:2:14,'XTickLabel', 0:2:);

    subplot(1,2,2)
    plot(vols,c2,'b--<',vols,c4,'r-*')
    xlabel('vols');
    ylabel('Concentration 2nd stage (g/L)');
    title('2stage profile')
    legend('Cr2-2000','Cr2-8000')
   %set(gca, 'XLim', [0, 14], 'XTick', 0:2:14,'XTickLabel', 0:2:14);

    figure
    subplot(1,2,1)
    plot(vols,nc1,'g-*',vols,nc3,'y-o')
```

```
    xlabel('vols');
    ylabel('Normalized Concentration (C/C0)');
    title('Normalized_concentrations profile');
    legend('Cr1-2000','Cr1-8000')
    %set(gca, 'XLim', [0, 14], 'XTick', 0:2:14,'XTickLabel', 0:2:14);

    subplot(1,2,2)
    plot(vols,nm1,'g-*',vols,nm3,'y-o')
    xlabel('vols');
    ylabel('Normalized Mass (M/M0)');
    title('Normalized_mass profile');
    legend('Mr1-2000','Mr1-8000')
    %set(gca, 'XLim', [0, 14], 'XTick', 0:2:14,'XTickLabel', 0:2:14);

    figure
    plot(vols,yield2,'b--<',vols,purity2,'k-o')
    ylim([40 100])
    xlabel('vols');
    ylabel('yield and purity (%)');
    title('two stage diafiltration')
    legend('yield','purity')
    %set(gca, 'XLim', [0, 14], 'XTick', 0:2:14,'XTickLabel', 0:2:14);

   hold off
end %###############

function dxdt=odetest(tactual,xactual)

            V0=0.200; %feed tank volume in L
            V1=V0+0.1;%0.100+0.100; % 100 mL feed tank+ 100 mL
membrane1
            V2=0.1;
            A=0.0014;%m2
            J= 8;%L/(m2 h bar)
            p= 20;%bar
            F1= J*A*p; %L/h
            rc=0.5; %rc=F3/F1
            F3= rc*F1;
            F2= F1-F3;%(F1=F2+F3) ;

    R1i=0.7995; %i= PEG2000 small residues need to be washed out
    R1j=0.9668; %j= PEG8000 Hub 1st coupling needs to be retained by
the membrane
    R2i=R1i;
    R2j=R1j;

    Cri1= xactual(1); %(g/L)
    Crj1= xactual(3); %(g/L)
    Cr2i= xactual(2); %(g/L)
    Cr2j= xactual(4); %(g/L)

    dxdt(1,1)= (1/V1)*(-F1*xactual(1)*(1-R1i)+F3*xactual(2));
    dxdt(2,1)= (1/V2)*(F1*xactual(1)*(1-R1i)-F2*xactual(2)*(1-R2i)-
F3*xactual(2));
    dxdt(3,1)= (1/V1)*(-F1*xactual(3)*(1-R1j)+F3*xactual(4));
    dxdt(4,1)= (1/V2)*(F1*xactual(3)*(1-R1j)-F2*xactual(4)*(1-R2j)-
F3*xactual(4));

end
```

7.2 The HPLC pump Plum flow Rate versus percentage of pump power

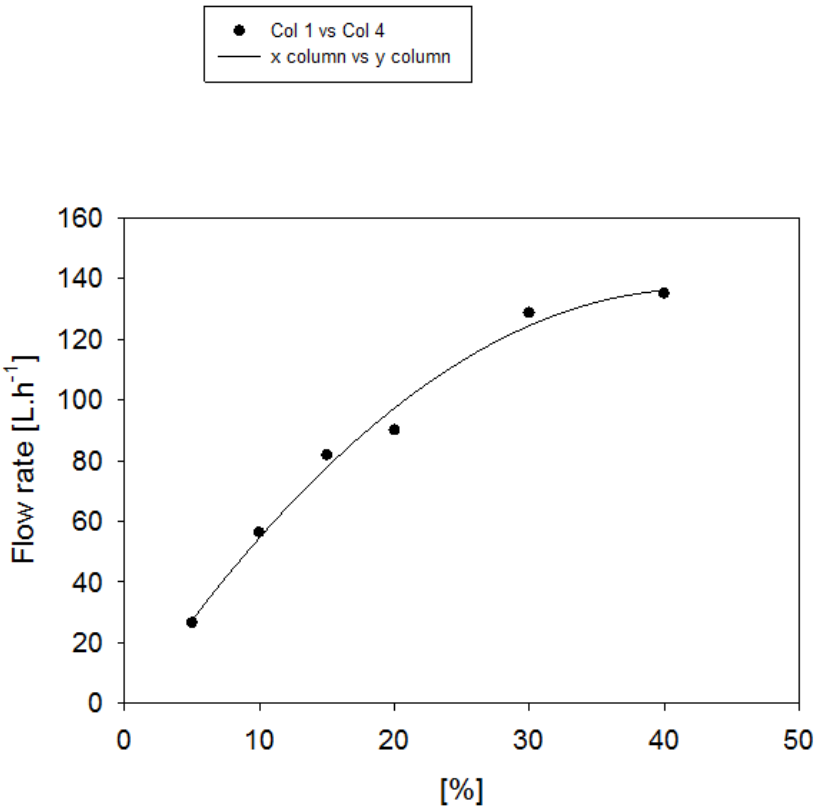

Figure 43. Plum flow Rate vs % of pump power